MOTS-c protects against placental injury via Nrf2 activation in hypoxia-induced intrauterine growth restriction mice

DAN CHEN[1*], HUI-MIN ZHAO[1*], XIAO-LIN SUN[2*], ZHI-XUAN XING[1], SHENG-PENG LI[1], SHUAI-CHAO LI[1], YA-XIAN WU[1], QING-FENG PANG[1] and JIAN-FENG HUANG[3]

[1]Department of Physiopathology, Wuxi School of Medicine, Jiangnan University, Wuxi, Jiangsu 214122, P.R. China; [2]Department of Neonatology, Maternal and Child Health Hospital of Linyi, Linyi, Shandong 276000, P.R. China; [3]Department of Radiation Oncology, Affiliated Hospital of Jiangnan University, Wuxi, Jiangsu 214122, P.R. China

Received May 9, 2025; Accepted October 23, 2025

DOI: 10.3892/ijmm.2025.5697

Abstract. Intrauterine growth restriction (IUGR) is a leading cause of perinatal morbidity and mortality. Oxidative stress is a key factor in the pathogenesis of IUGR. The transcription factor nuclear factor erythroid 2-related factor 2 (Nrf2) is a key regulator of the cellular antioxidant response. MOTS-c, a 16-amino acid peptide derived from the mitochondria, regulates oxidative stress related pathways. However, the effects of MOTS-c on IUGR remain unclear. The present study aimed to investigate the role of MOTS-c in hypoxia-induced placental restriction and IUGR and its underlying mechanisms. Wild-type and Nrf2 knockout (KO) maternal mice were exposed to hypoxia from gestational days 11 to 17.5 to establish the IUGR model. Human umbilical vein endothelial cells (HUVECs) were used for *in vitro* assays. Maternal serum and placenta MOTS-c concentration were measured using an enzyme-linked immunosorbent assay. Hematoxylin and eosin staining, reverse transcription-quantitative PCR, western blotting, immunohistochemistry and immunofluorescence techniques were employed to evaluate the effects of MOTS-c treatment on IUGR. It was found that reduced placental content of MOTS-c was positively correlated with low fetal weight in mice with hypoxia-induced IUGR. The administration of MOTS-c (5 mg/kg) significantly attenuated hypoxia-induced IUGR by promoting placental angiogenesis and inhibiting oxidative stress-mediated placental dysfunction. Furthermore, these protective effects exerted by MOTS-c were dependent on Nrf2 activation, as administration of MOTS-c had no protective role in Nrf2 KO mice or HUVECs pre-treated with ML385, a Nrf2 inhibitor. Taken together, the present study demonstrated that MOTS-c mitigated placental injury in hypoxia-induced IUGR by activation of the Nrf2 signaling pathway, thus potentially identifying a novel therapeutic strategy for hypoxia-induced IUGR.

Correspondence to: Professor Qing-Feng Pang, Department of Physiopathology, Wuxi School of Medicine, Jiangnan University, 1800 Lihu Avenue, Binhu, Wuxi, Jiangsu 214122, P.R. China
E-mail: qfpang@jiangnan.edu.cn

Dr Jian-Feng Huang, Department of Radiation Oncology, Affiliated Hospital of Jiangnan University, 1000 Hefeng Road, Wuxi, Jiangsu 214122, P.R. China
E-mail: 9862019007@jiangnan.edu.cn

*Contributed equally

Abbreviations: GD, gestational day; HUVEC, human umbilic vein endothelial cells; IUGR, intrauterine growth restriction; MDA, malondialdehyde; Nrf2, nuclear factor erythroid 2-related factor 2; ROS, reactive oxygen species; SOD, superoxide dismutase; VEGFA, vascular endothelial growth factor A; VEGFR2, VEGF receptor 2

Key words: MOTS-c, nuclear factor erythroid 2-related factor 2, placental injury, hypoxia, intrauterine growth restriction

Introduction

Intrauterine growth restriction (IUGR), also known as fetal growth restriction, is defined as a condition in which a fetus is small for gestational age (SGA) and falls below the 10th percentile for gestational age and sex. (1). In 2020, one in five newborns worldwide (23.4 million) were SGA, a condition linked to ~20% of term stillbirths (2). Maternal nutrition and stress during pregnancy, such as high-altitude pregnancy, smoking and preeclampsia, can lead to adverse effects (3,4). Among these, antenatal hypoxia-induced placental insufficiency has been identified as a primary risk factor for stillbirths, neonatal deaths and perinatal morbidity associated with IUGR (5-7). Antioxidant supplementation has been attempted to treat IUGR, but has not achieved success (8,9). Therefore, it remains crucial to discover new and efficacious treatments for IUGR.

The 16-amino acid mitochondria-derived peptide, MOTS-c, is synthesized by encoding a compact open reading frame located within the genomic sequence of the mitochondrial 12S ribosomal RNA gene (10). It has been reported that MOTS-c induces transcription of antioxidant genes and enhances cellular resistance to oxidative stress injury (11). Low plasma levels of MOTS-c are associated with endothelial mitochondrial dysfunction in patients with obesity and coronary artery disease (12,13). MOTS-c serves key roles in the onset and development of cardiovascular diseases, aging and age-related diseases (14,15). In addition, supplementation

with MOTS-c inhibits oxidative stress in rotenone-induced neuron degeneration (13), diabetic cardiomyopathy (16) and diabetic nephropathy (17). However, the role of MOTS-c in hypoxia-induced IUGR remains unclear.

The placenta possesses a diverse range of antioxidant defense systems that effectively mitigate the accumulation of reactive oxygen species (ROS). Among these systems, the nuclear factor erythroid 2-related factor 2 (Nrf2) pathway serves a pivotal role in governing oxidative stress-associated disorders (18). Nrf2 is typically bound to Kelch-like ECH-associated protein 1 (KEAP1) in the cytoplasm, but dissociates upon exposure to ROS and moves into the nucleus where it activates genes associated with antioxidant defense mechanisms (19). Furthermore, the KEAP1-Nrf2 pathway is also activated by aerobic exercise or MOTS-c (20). We previously demonstrated that MOTS-c could directly increase synthesis of Nrf2 independent of protein degradation and promote Nrf2 nucleus translocation (21,22). During pregnancy, Nrf2 protects the fetus from adverse oxidative stress conditions by ensuring proper placental function (23). Evidence suggests that Nrf2 deficiency leads to reduced fetal weight and placental volume (24). However, it remains unclear whether MOTS-c regulates oxidative stress in IUGR via activation of the Nrf2-mediated anti-oxidative pathway. The present study aimed to investigate whether MOTS-c alleviates hypoxia-induced placental restriction and IUGR by activating the Nrf2 signaling pathway.

Materials and methods

Animals. A total of 69 C57BL/6 wild-type mice (46 female and 23 male), aged 6-8 weeks, and weighing 18-20 g, were sourced from the Jiangnan University Laboratory Animal Center (Wuxi, China). Nrf2 knockout (KO) mice were obtained from the Model Animal Research Institute of Nanjing (Nanjing, China). These mice were housed in a specific pathogen-free facility environment, which maintained an ambient humidity of 50% and a temperature range of 22-25˚C. The mice had free access to food and water and were subjected to a 12-h light-dark cycle managed by an automated light control system. All animal experiments were approved by the Animal Experimentation Ethics Committee of Jiangnan University [approval nos. 2 0220930m1080501(383) and 20231115m1080530(555)]. All animal experiments were performed in accordance with guidelines established by the International Association for the Assessment and Accreditation of Laboratory Animal Care (25) and the relevant laws of the National Research Council's Guide for the Care and Use of Laboratory Animals.

IUGR mouse model establishment and sample collection. Females were paired with males (with a total of 23 pairs) overnight for mating purposes, and the day of observation of a vaginal plug was designated as gestational day (GD) 0. The IUGR mouse model was established as previously reported (26,27) and as similarly described in our previous studies (28,29). Briefly, 17 pregnant mice were housed under hypoxic conditions (FiO_2=0.105) from GD 11 to GD 17.5, which refers to IUGR group. The control group of pregnant mice were housed under normoxic conditions (FiO_2=0.21) throughout pregnancy. To determine the protective effects of MOTS-c, randomly selected control and IUGR pregnant mice received intraperitoneal injections of 5 mg/kg MOTS-c once a day from GD 11 to 17.5 (10,30,31), which refers to the MOTS-c (n=6) and IUGR + MOTS-c groups (n=5), respectively. Meanwhile, control and IUGR mice were injected with an equivalent volume of physiological saline from GD 11 to 17.5, which refers to the normal group (n=6) and IUGR group (n=6) respectively. No suitable drug is presently available for use as a positive control in the treatment of hypoxia-induced IUGR (8,9), therefore, no positive control group was included.

To explore the protective mechanisms of MOTS-c, pregnant C57BL/6 mice and Nrf2 knockout (KO) mice were randomly divided into six groups: Normal (n=6), $Nrf2^{-/-}$ (n=4), IUGR (n=6), IUGR + MOTS-c (n=5), $Nrf2^{-/-}$ + IUGR (n=4), and $Nrf2^{-/-}$ + IUGR + MOTS-c (n=5). MOTS-c (5 mg/kg) was intraperitoneally injected daily from GD 11 to 17.5, with an equivalent volume of physiological saline injected as the loading control. On GD 17.5, each pregnant mouse was terminally anesthetized using pentobarbital sodium (50 mg/kg, intraperitoneally) as previously reported (32,33). The maternal blood was collected according to our previous study (34). Briefly, the mice were fixed in a supine position. After making a sternal incision, blood was collected by inserting a 26-G needle vertically through the second intercostal space into the heart, using a vacuum tube system. The blood was incubated at room temperature for 30 min, centrifuged at 105.45 x g for 10 min at 4˚C and then the separated serum was used for the study. Finally, the mice were then euthanized via cervical dislocation, and death was confirmed by the absence of a heartbeat and cessation of breathing. After euthanizing the dams, caesarean section surgery was performed via hysterectomy as according to a previous study (35). Briefly, the abdomen was sterilized with 70% ethanol and an abdominal incision was made to retrieve the uterus, which was transferred onto a sterile gauze over a heating pad. Finally, the pups were extracted by incising the uterine wall and applying gentle pressure. Fetuses and placentas were then collected. The total number of fetuses were counted, and the weight of the fetuses and placentas were measured. The placental efficiency was calculated as follows: Placental efficiency (%)=(fetal weight/placental weight) x 100 (36). Fetal pups were anesthetized by inhalation of 2% isoflurane and sacrificed via cervical dislocation. Euthanasia was confirmed by the absence of heartbeat under the dissecting microscope, with the tissue appears pale. Placental tissues were collected for subsequent experiments; all collected samples were stored at -80˚C until use.

Synthesis of MOTS-c peptides. The human MOTS-c peptide was synthesized by the Mimotopes Pty Ltd., using 9-fluorenylmethoxycarbonyl solid-phase chemistry in accordance with standard peptide synthesis protocols (37). The synthesized peptide had purity >95%, as determined through high-performance liquid chromatography by Mimotopes Pty Ltd. The amino acid sequence of MOTS-c was as follows: Met-Arg-Trp-Gln-Glu-Met-Gly-Tyr-Ile-Phe-Tyr-Pro-Arg-Lys-Leu-Arg. The MOTS-c peptide was dissolved in distilled deionized water at a concentration of 1 mg/ml and stored at -20˚C.

Histopathological staining. Placental tissues were fixed in a 4% paraformaldehyde solution at room temperature for 48 h,

and embed in paraffin and sectioned (4-μm thick). The sections were stained with hematoxylin and eosin (cat. no. D006-1, Nanjing Jiancheng Bioengineering Institute). Briefly, the sections were stained with Harris's hematoxylin (0.1%) for 6 min, differentiated with 1% acid ethanol, rinsed and blued with tap water, following counterstaining with eosin Y (0.5-1%) for 1 min at room temperature. Images of placenta sections were captured using a Panoramic MIDI scanner (3DHISTECH Ltd.; magnification, x20) and for each sample, ~10 images were acquired. Imaging and quantification were performed blinded. The area of the segmented blood sinusoid regions was quantified using the area measurement tool of the ImageJ software version 1.53k (National Institutes of Health). Data on the areas of blood sinusoids were statistically analyzed to calculate the means and standard deviation. The assessment of placental angiogenesis was performed by quantifying the sinusoidal areas.

Immunohistochemical staining. To detect intracellular antigens, the placental sections (4-μm thick) were deparaffinized at 65˚C for 60 min and rehydrated using gradient alcohol. Antigen retrieval was performed using tris-EDTA buffer at 98˚C for 25 min, followed by permeabilization with 0.1% Triton X-100 in PBS for 15 min at room temperature. To minimize non-specific binding, sections were blocked with 5% normal goat serum (cat. no. A7906; MilliporeSigma) for 2 h at room temperature. For HRP-based assays, endogenous peroxidases were quenched with 3% hydrogen peroxide in methanol for 15 min before blocking. The placental sections were then incubated with the primary antibodies against CD31 (1:100; cat. no. #77699s; Cell Signaling Technology) and MOTS-c (1:100; cat. no. #MOTSC-101AP; FabGennix International Inc.) overnight at 4˚C. At room temperature, the samples were co-incubated with the corresponding fluorescence labeled secondary antibody (1:100; cat. no. 33106ES60; Shanghai Yeasen Biotechnology Co., Ltd.) for 60 min, and freshly prepared DAB (cat. no. #CW20695; CWBIO) staining was then performed. Finally, sections were counterstained with hematoxylin (cat. no. I030-1; Nanjing Jiancheng Bioengineering Institute), dehydrated and cleared. Images were captured using Panoramic MIDI (3D HISTECH Ltd.) and analyzed using the Panoramic Viewer software version 2.1 (3DHISTECH Ltd.).

Enzyme linked immunosorbent assay (ELISA). MOTS-c content in the serum and placental tissues of the pregnant mice was quantified using an ELISA kit (cat. no #MM-46300M1; Jiangsu Meimian Industrial Co., Ltd.) following the manufacturer's guidelines.

Cell culture and treatments. The immortalized human umbilical vein endothelial cells (HUVECs) and human placental trophoblast cell (HTR-8/SVneo) were obtained from The Cell Bank of Type Culture Collection of The Chinese Academy of Sciences. These cells were cultured in Dulbecco's Modified Eagle's Medium (DMEM; cat. no. 319-005-CL; Wisent, Inc.) enriched with 10% fetal bovine serum (FBS; cat. no. 40130ES76; Shanghai Yeasen Biotechnology Co., Ltd.) and 1% penicillin-streptomycin mixture (cat. no. C0222; Beyotime Institute of Biotechnology). Incubation conditions were set to a humidified atmosphere at 37˚C and 5% CO_2.

In investigating the effects of MOTS-c on hypoxia-induced HUVECs and HTR-8/SVneo cells, the cells were pre-treated with 10 μM MOTS-c under normoxic conditions (21% O_2) or an equivalent volume of phosphate buffer saline (PBS), followed by modeling under hypoxic conditions for 48 h; the use of 1% O_2 is a well-established model in the *in vitro* study of hypoxia-related diseases, and has been demonstrated to cause dysregulation of angiogenesis and proliferation in HUVECs as previously described (38). To mimic the abnormal angiogenesis under hypoxia exposure, HUVECs were exposed to an oxygen concentration of FiO_2=0.01 for 48 h. The procedure for each experimental approach was standardized to ensure consistent operational steps and treatment conditions across three replicates. HUVECs and HTR-8/SVneo cells used were confined to those within the 3rd to 5th passages for experimental consistency and reliability. The experiment was independently repeated for three times.

To determine the role of Nrf2 in hypoxia-stimulated HUVECs, ML385 (cat. no. HY-100523; MedChemExpress), a specific Nrf2 inhibitor was used as previously reported (39). Briefly, HUVECs were stimulated with ML358 (5 μM) for 1 h, followed by administration with MOTS-c (10 μM) for 2 h and exposed to hypoxia (1% O_2) for an additional 48 h.

Optical Microscopy. For morphological assessment, HUVECs were examined under a phase-contrast microscope equipped with a digital camera (DP11, Olympus), and images were documented.

Cell viability assay. Cell viability was evaluated by the Cell Counting Kit-8 (CCK-8) assay (cat. no. C0037; Beyotime Institute of Biotechnology). Cells were seeded at a density of $1x10^4$ cells/well in 96-well plates. After rinsing with PBS, the cells were exposed to CCK-8 solution (1:10 dilution). The cells were incubated at 37˚C for 2 h, and then the absorbance were measured at 450 nm using a microplate reader (BioTek; Agilent Technologies, Inc.).

Nrf2 overexpression in HUVECs. The Nrf2 overexpression plasmid was constructed and obtained from OBiO Technology (Shanghai) Corp., Ltd. Briefly, after reaching 80% confluence, the cells were transfected with pcDNA3.1 plasmid or Nrf2 overexpression plasmids (1 μg/ml) using a transfection reagent (cat. no. C10511-05; Guangzhou RiboBio Co., Ltd.) and cultured at 37˚C and 5% CO_2. After 24 h, the medium was changed and exposed to normoxic (21% O_2) or hypoxic (1% O_2) conditions for 48 h. Cells were then harvested for downstream analysis, with Nrf2 overexpression verification performed by reverse transcription-quantitative PCR (RT-qPCR).

Nrf2 siRNA transfection in HUVECs. Nrf2 siRNA was obtained from KeyGEN BioTECH. Briefly, after reaching 80% confluence, HUVECs cells were transfected with control siRNA (20 μM) or Nrf2 siRNA (20 μM) using a transfection reagent (cat. no. C10511-05; Guangzhou RiboBio Co., Ltd.) according to the manufacturer's instructions. After 12 h, the medium was changed and the cells were cultured for 36 h at 37˚C and 5% CO_2. Cells were then harvested for downstream analysis, with Nrf2 knockdown verification performed by RT-qPCR. The siRNA sequences used were as follows: Nrf2

sense (S), 5'-GCAGCAAACAAGAGAUGGCAAdTdT-3' and anti-sense (AS), 5'-UUGCCAUCUCUUGUUUGCUGCdTdT-3'; and negative control siRNA (vector-siRNA) S, 5'-UUCUCCGAACGUGUCACGUdTdT-3' and AS, 5'-ACGUGACACGUUCGGAGAAdTdT-3'.

ROS measurements. The ROS production in HUVECs and HTR-8/SVneo cells were assessed using 2',7'-dichlorodihydro fluorescein diacetate (DCFH-DA) diacetyldichlorofluorescein staining solution (1:1,000; cat. no. E004-1-1; Nanjing Jiancheng Bioengineering Institute) in the dark at 37˚C for 15 min, and analyzed with a Zeiss fluorescence microscope (Zeiss AG). The mitochondrial ROS levels were assessed using MitoSOX (cat. no. #40778ES50; Shanghai Yeasen Biotechnology Co., Ltd.). The cells were treated with a MitoSOX working solution (5 mM) at 37˚C for 20 min. Then, the ROS fluorescence intensity was visualized using a confocal microscope (Zeiss AG).

Immunofluorescence staining. For Nrf2 immunofluorescence staining in HUVECs, cells were fixed with 100% methanol for 15 min at -20˚C, followed by permeabilization with 0.1% Triton X-100 for 10 min and blocked with 1% bovine serum albumin (BSA) (cat. no. HY-D0842; MedChemExpress) for 60 min at room temperature. The cells were then incubated with Nrf2 antibody (cat. no. #ab62352; Abcam) at 1/100 dilution overnight at 4˚C followed by a further incubation with Alexa 488-conjugated secondary antibody (1:200; cat. no. 33103ES60; Shanghai Yeasen Biotechnology Co., Ltd.) at room temperature for 1 h. The Nrf2 antibody specificity was validated by Nrf2 siRNA knockdown (Fig. S1). The nuclei were labelled with DAPI solution (1 mg/ml; cat. no. #P0131; Beyotime Institute of Biotechnology) for 10 min at room temperature. Images were captured using a confocal microscope.

For Ki-67 and Nrf2 immunofluorescence staining in placental tissues, the sections were permeabilized with 0.1% Triton X-100 for 10 min and blocked with 5% BSA (cat. no. HY-D0842; MedChemExpress) for 2 h at room temperature. The samples were incubated with primary antibodies anti-Ki-67 (1:100; cat. no. #9129; Cell Signaling Technology, Inc.) and anti-Nrf2 (1:100; cat. no. #62352; Abcam) overnight at 4˚C, followed by incubation with secondary antibodies conjugated to Alexa Fluor 488 (cat. no. #33103ES60; 1:200; Shanghai Yeasen Biotechnology Co., Ltd.) or Alexa Fluor 594 (cat. no. #33112ES60; 1:200; Shanghai Yeasen Biotechnology Co., Ltd.). Subsequently, the nuclei were stained with DAPI (1 μg/ml; cat. no. HY-D1738; MedChemExpress) for 5 min at room temperature. Images were acquired using a Zeiss Axio Imager 2 fluorescent microscope (Carl Zeiss AG). The number of immunoreactivity positive cells was quantified as the percentage of total cells. All samples were blinded during imaging and quantification.

Tube formation assay. Matrigel (50 μl; cat. no. #082704; Shanghai Nova Pharmaceutical Technology Co., Ltd) was added to each well of 96-well plates and allowed to solidify in a cell incubator at 37˚C with 5% CO_2 for 60 min. Next, $3x10^4$ HUVECs in 100 μl of DMEM containing 5% fetal bovine serum (cat. no. 40130ES76; Shanghai Yeasen Biotechnology Co., Ltd.) and 1% penicillin-streptomycin (cat. no. C0222; Beyotime Institute of Biotechnology). were added to each well. After 6 h of incubation, tubular structures were examined and visualized using a Zeiss Axio Imager 2 fluorescent microscope (Carl Zeiss AG), and the tube lengths were quantified using ImageJ software version 1.53k (National Institutes of Health). The angiogenic capability was quantified by measuring the number of tubes and the mean mesh size per field from three randomly selected fields per well.

L-lactate dehydrogenase (LDH), superoxide dismutase activity (SOD) and malondialdehyde (MDA) content. LDH concentration, SOD activity and the MDA content were quantified in the serum of pregnant mice and HUVECs using kits from Nanjing Jiancheng Bioengineering Institute (LDH kit, cat. no. A020-2; SOD kit, cat. no. A001-3-2: MDA kit, cat. no. A003-1-2) following the manufacturer's protocols.

Determination of mitochondrial membrane potential (MMP). The MMP was assessed using JC-1 dye (Beyotime Institute of Biotechnology). Briefly, JC-1 dye added to the cell suspension to achieve a final dye concentration of 10 μM. The cells were incubated with the JC-1 dye mixture at 37˚C for 15 min to allow the dye to enter the cells and accumulate in the mitochondria. JC monomers (488 nm) and JC aggregates (570 nm) were visualized using a fluorescence microscope (Olympus Corporation), and images were acquired from a random selection of 3-4 fields per well.

Western blotting. Placentas and HUVEC cells were lysed using RIPA buffer (cat. no. P0013B; Beyotime Institute of Biotechnology) containing with protease and phosphatase inhibitors (cat. no. P1045; Beyotime Institute of Biotechnology). Nuclear and cytoplasmic extracts from placental tissues were prepared using a Nuclear Extraction Kit (cat. no. W037-1-1; Nanjing Jiancheng Bioengineering Institute) according to the manufacturer's instructions. The protein concentrations were determined according to the manufacturer instructions using a BCA Protein Assay kit (cat. no. P0009; Beyotime Institute of Biotechnology). Subsequently, the lysates were separated on 8 and 10% SDS-PAGE gels and transferred onto polyvinylidene difluoride membranes (cat. no. P2938; MilliporeSigma; Merck KGaA). Following a 2 h blocking step at room temperature with 5% BSA (cat. no. HY-D0842; MedChemExpress) in Tris-buffered saline, the membranes were incubated overnight at 4˚C with primary antibodies targeting CD31 (1:1,000; cat. no. 77699s; Cell Signaling Technology, Inc.), vascular endothelial growth factor receptor 2 (VEGFR2; 1:1,000; cat. no. 26415-1-AP; Proteintech), vascular endothelial growth factor A (VEGFA; 1:1,000; cat. no. 66828-1-Ig; Proteintech), Nrf2 (1:1,000; cat. no. 62352; Abcam) and glyceraldehyde-3-phosphate dehydrogenase (GAPDH; 1:5,000; cat. no. 263962; Abcam). After washing, the membranes were incubated with secondary antibodies for 2 h at room temperature (Goat Anti-Mouse IgG, 1:5,000; cat. no. CW0102S; Goat Anti-Rabbit IgG, 1:5,000; cat. no. CW0103S; Jiangsu CoWin Biotech Co., Ltd.) corresponding to the primary antibody source. Protein bands were visualized using a ChemiDocTM XRS Plus luminescence image analyzer (Bio-Rad Laboratories, Inc.) with an ECL

system (MilliporeSigma; Merck KGaA), and quantified using ImageJ software version 1.53k (National Institutes of Health).

Reverse transcription quantitative-polymerase chain reaction (RT-qPCR). Total RNA from the placental tissue was extracted using TRIzol Reagent (cat. no. R401; Vazyme Biotech Co., Ltd.) and then reverse-transcribed into complementary DNA using a PrimeScript RT Reagent Kit (cat. no. R323; Vazyme Biotech Co., Ltd.) according to the manufacturer's protocol. Target mRNA amplification was measured using SYBR Premix Ex Taq™ (cat. no. 11201ES08; Shanghai Yeasen Biotechnology Co., Ltd.) with a LightCycler® 480 detection PCR system (Roche Diagnostics). The PCR amplification protocol consisted of an initial denaturation step at 95˚C for 5 min, followed by 40 cycles of denaturation at 95˚C for 10 sec, annealing at 55˚C for 20 sec and extension at 72˚C for 20 sec. Quantification was performed employing the $2^{-\Delta\Delta Cq}$ method (40), with GAPDH serving as the reference gene. The primer sequences are provided in Table I.

Statistical analyses. Statistical data are depicted as means ± standard deviation. The D'Agostino-Pearson test and Shapiro-Wilk test were used for normality tests. For quantitative data obeying normal distribution, comparisons between two groups were performed using Student's unpaired two-tailed t-test. To compare among ≥3 groups, the Brown-Forsythe analysis was used to test for homogeneity of variance, if the variance was homogeneous, the Tukey's test of one-way analysis of variance was used. If variances were not homogeneous, Dunnett's T3 test was used to test for differences between multiple groups. The association between different targets was analyzed using Pearson's correlation test. Analyses were performed using the GraphPad Prism software (version 8.0.2; Dotmatics). $P<0.05$ was considered to indicate a statistically significant difference.

Table I. Primers for reverse-transcription quantitative PCR analysis.

A, Mouse primers

Gene	Sequence (5'-3')
Pgf	F: AGTGGAAGTGGTGCCTTTCAA
	R: GTGAGACACCTCATCAGGGTA
Fatp4	F: ACTGTTCTCCAAGCTAGTGCT
	R: GATGAAGACCCGGATGAAACG
Glut1	F: TCAAACATGGAACCACCGCTA
	R: AAGAGGCCGACAGAGAAGGAA
Snat2	F: GGGACATAAGGCGTATGGTCT
	R: GGTAGCTTGACATAGCCCCAA
Igf2	F: CGTGGCATCGTGGAAGAGT
	R: ACGTCCCTCTCGGACTTGG
Nrf2	F: TCTTGGAGTAAGTCGAGAAGTGT
	R: GTTGAAACTGAGCGAAAAAGGC
Gapdh	F: AGGTCGGTGTGAACGGATTTG
	R: GGGGTCGTTGATGGCAACA

B, Human primers

Gene	Sequence (5'-3')
VEGFA	F: AGGGCAGAATCATCACGAAGT
	R: AGGGTCTCGATTGGATGGCA
VEGFR2	F: GGCCCAATAATCAGAGTGGCA
	R: CCAGTGTCATTTCCGATCACTTT
CD31	F: CCAAGGTGGGATCGTGAGG
	R: TCGGAAGGATAAAACGCGGTC
GAPDH	F: GGAGCGAGATCCCTCCAAAAT
	R: GGCTGTTGTCATACTTCTCATGG

F, forward; R, reverse; Pgf, placental growth factor; Igf2, insulin-like growth factor 2; Glut1, glucose transporter type 1; Fatp4, fatty acid transporter 4; Snat2, sodium-dependent neutral amino acid transporter-2; VEGFA, vascular endothelial growth factor A; VEGFR2, VEGF receptor 2; Nrf2, nuclear factor erythroid 2-related factor 2.

Results

Decreased levels of MOTS-c in the serum and placenta of pregnant mice is associated with reduced fetal weight and lower placental vascular density. Exposure to hypoxia during pregnancy led to significant fetal growth restriction (Fig. 1A), evidenced by reduced fetal body weight and diminished placental efficiency (the fetal-to-placental weight ratio; Table II). Additionally, the blood sinus areas within the placenta were significantly reduced in IUGR mice (Fig. 1B and C). The expression levels of CD31, a vascular marker, were significantly lower in the placenta of IUGR mice compared with that of the Controlgroup (Fig. 1D and E). These findings suggested a reduction in placental vascular density following antenatal maternal hypoxia exposure. MOTS-c content was significantly reduced in both maternal serum and placenta after hypoxic exposure (Fig. 1F and G), further validated by immunohistochemistry of placental tissues, with 34.8% reduction of MOTS-c positive cells in IUGR mice when compared with the control group (Fig. 1H and I). Furthermore, placental MOTS-c levels exhibited a positive correlation with fetal mouse weight ($R^2=0.4010$; $P=0.0382$; Fig. 1J). These data suggested that the decreased fetal weight and placental vascular density resulting from antenatal maternal hypoxia may be associated with reduced MOTS-c content.

MOTS-c promotes placental angiogenesis and increased fetal weight in IUGR mice. To assess the potential benefits of MOTS-c supplementation on fetal growth, synthetic MOTS-c peptide was administered intraperitoneally. The timeline of this experimental study is schematically presented in Fig. 2A. This intervention resulted in a significant increase in maternal serum and placental MOTS-c content, as showed in Fig. S2A-D. When compared with that of the normal group, the MOTS-c group mice showed no significant differences in fetal growth, as indicated by normal size, morphology and fetal weight (Fig. S3A and B), fetal weight of the MOTS-c group remained normal for up to 4 weeks after birth (Fig. S3C). Therefore, subsequent investigations focused solely on the effects of MOTS-c on IUGR mice. MOTS-c administration significantly improved fetal development, with increased fetal size and fetal weight

Table II. Descriptive statistics of dams and fetuses exposed to hypoxia.

Characteristic	Normal	IUGR	P-value
Maternal body weight, g	31.9±1.1	29.6±1.3[a]	0.0087
Litter size	7.6±1.4	7.4±1.6	0.8626
Litter parameters, n	53	52	
Fetal weight (g)	0.90±0.085	0.49±0.075[b]	<0.0001
Crown-rump length (mm)	8.6±0.4	8.0±0.4	0.0333
Placenta, n	53	52	
Placenta weight (g)	0.0772±0.0102	0.0836±0.00790	0.2954
Fetal/weight ratio	11.8±2.0	6.0±1.2[b]	0.0001

[a]P<0.01; [b]P<0.001. Data are presented as mean ± SD. IUGR, intrauterine growth restriction.

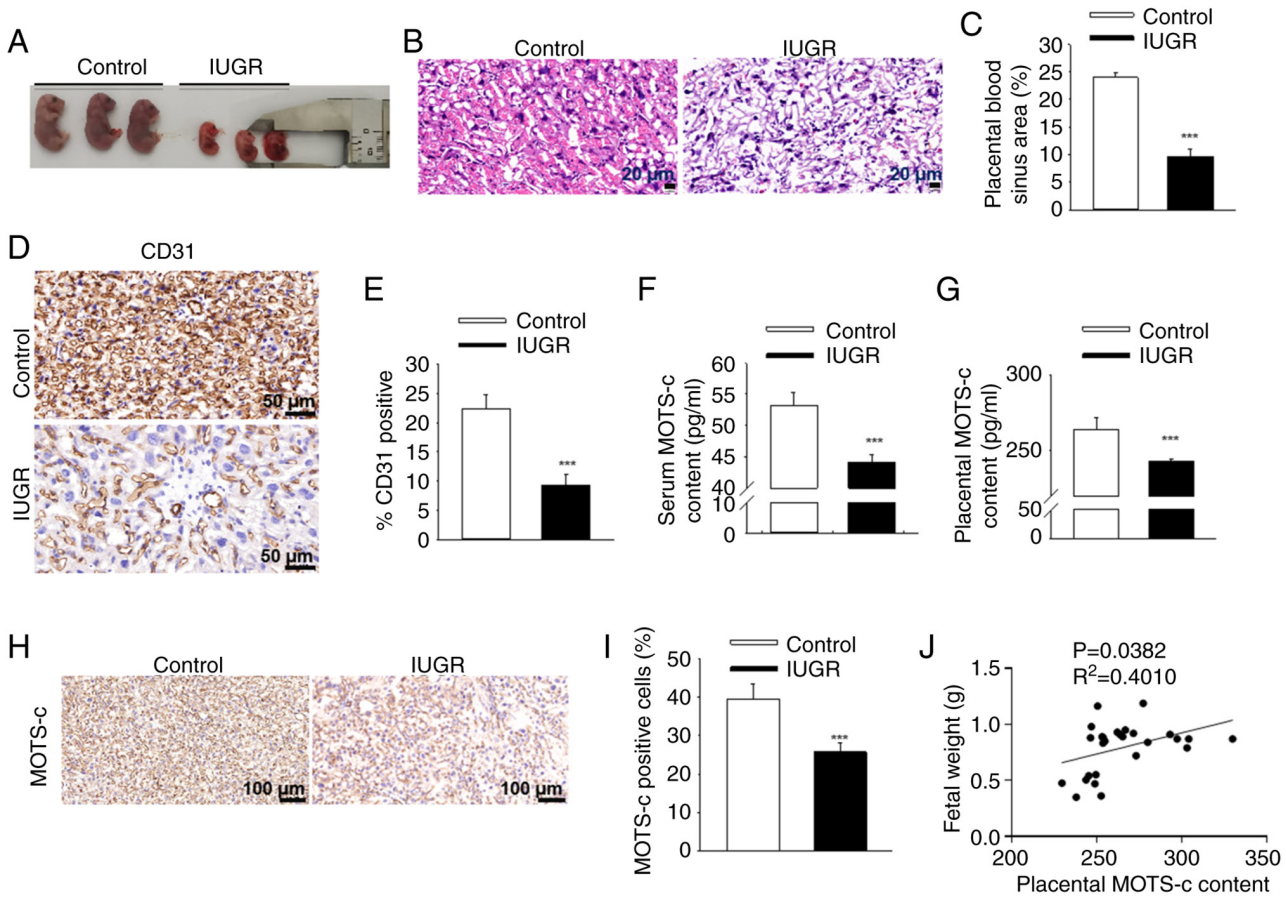

Figure 1. Decreased MOTS-c expression levels are associated with low fetal weight in hypoxia-induced IUGR mice. (A) Morphology of normal and IUGR fetal mice on GD17.5. (B) Representative images of H&E staining of placental tissues. Scale bar, 20 μm. (C) Quantification of placental blood sinus area. (D) Representative IHC images of CD31. Scale bar, 50 μm. (E) Quantification of the CD31 positive area of IHC images. (F) Maternal serum MOTS-c content and (G) Placental MOTS-c content. (H) Representative IHC images of MOTS-c in placenta. Scale bar, 100 μm. (I) Quantification of the MOTS-c positive area of IHC images. (J) Pearson's correlation coefficient analysis of the MOTS-c content with fetal mouse weight. Data are expressed as the mean ± SD, n=6. ***P<0.001 vs. Control. IUGR, intrauterine growth restriction; GD, gestational day; IHC, immunohistochemistry.

compared with that of the IUGR group (Fig. 2B and C). Furthermore, the ratio of fetal to placental weight was significantly increased following MOTS-c administration in the IUGR mice compared with the untreated IUGR mice (Fig. 2D). In addition, MOTS-c administration significantly improved blood sinus areas (Fig. 2E and F) and upregulated CD31 expression in the placenta in the IUGR + MOTS-c group compared with that of the IUGR group (Fig. 2G and H). These findings suggested beneficial effects of MOTS-c treatment against hypoxia-induced poor placental vascular density and subsequent fetal development. As the VEGF pathway is recognized as a major regulatory mechanism governing developmental angiogenesis (41), the expression levels of VEGFA and VEGFR2 were investigated.

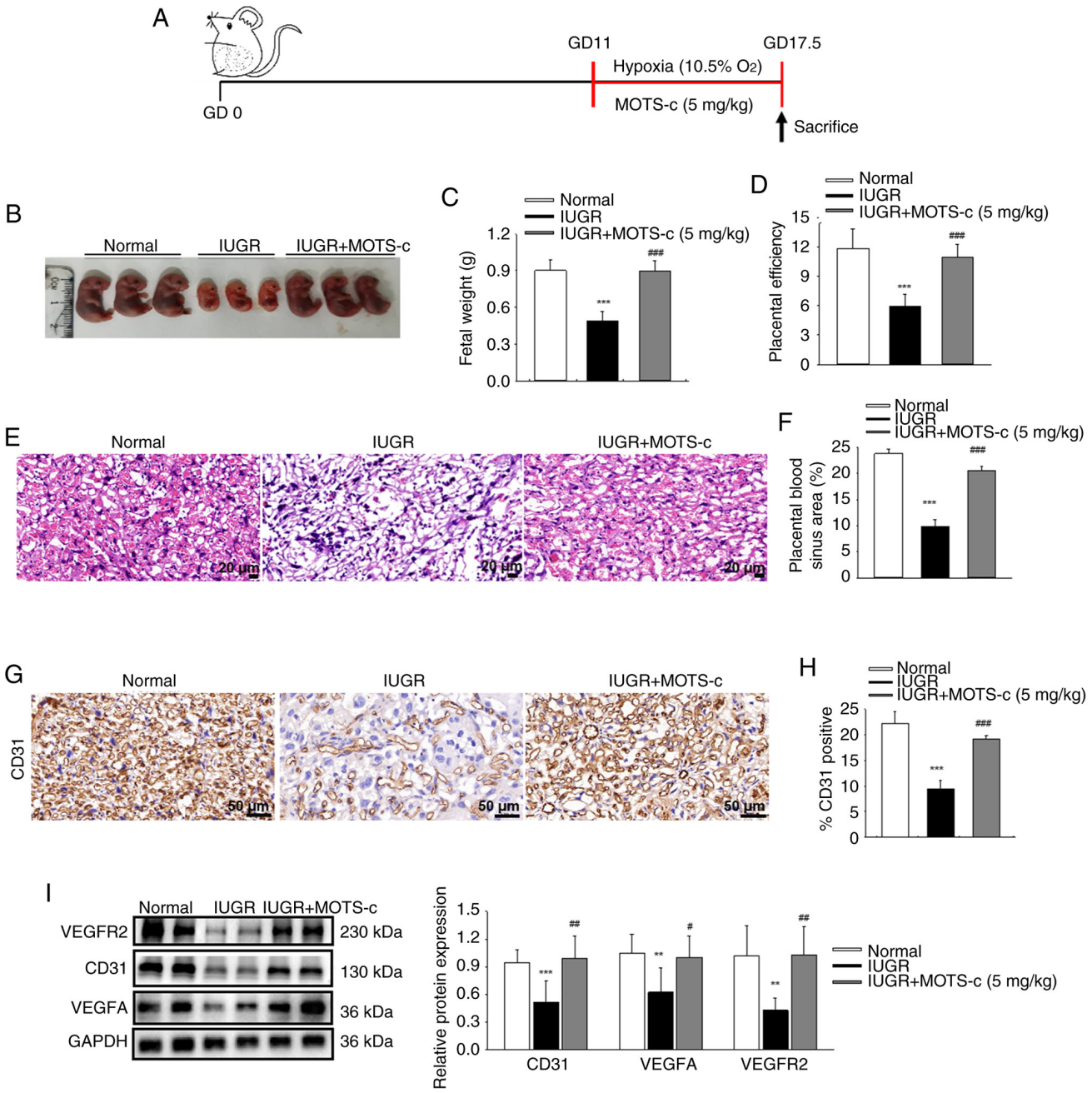

Figure 2. MOTS-c administration protects against hypoxia-induced fetal growth restriction. (A) Schematic timeline of the experimental setup. (B) Morphology of fetal mice on GD17.5. (C) Mean fetal weights within each litter. (D) Placental efficiency, which represents the ratio of fetal to placenta weight. (E) Representative images of H&E staining of placental tissues. Scale bar, 20 μm. (F) Quantification of placental blood sinus area. (G) Representative IHC images CD31. Scale bar, 50 μm. (H) Quantification of CD31 positive area. (I) Western blotting analysis of CD31, VEGFA and VEGFR2 protein expression in placenta. Data are expressed as the mean ± SD. Normal, n=6; IUGR, n=6; IUGR + MOTS-c, n=5. **P<0.01 vs. normal, ***P<0.001 vs. normal; $^{\#}$P<0.05 vs. IUGR; $^{\#\#}$P<0.01 vs. IUGR; $^{\#\#\#}$P<0.001 vs. IUGR. IUGR, intrauterine growth restriction; GD, gestational day; VEGFA, vascular endothelial growth factor A; VEGFR2, VEGF receptor 2.

The protein expressions levels of VEGFA and VEGFR2 were decreased in placental tissues following hypoxic exposure in the IUGR group, while in comparison, MOTS-c treatment significantly upregulated the VEGF pathway in the IUGR + MOTS-c group (Fig. 2I). These results suggested that MOTS-c improved hypoxia-induced IUGR by promoting placental angiogenesis.

Increased cell proliferation and upregulation of mRNA expression of nutrient transporter genes in placental tissues are associated with MOTS-c treatment. To investigate the role of MOTS-c on cell proliferation in placenta subjected to IUGR, placental tissues of the normal, IUGR and IUGR + MOTS-c group mice were stained with Ki-67, a marker for cell proliferation, and the number of positive cells was quantified. The concentration of Ki-67-positive cells were significantly decreased in hypoxia-exposed placental tissues compared with that in the normal group, which was subsequently reversed by MOTS-c administration (Fig. 3A and B). Furthermore, the mRNA expression levels of placental growth factor (*Pgf*), sodium-dependent neutral amino acid transporter-2 (*Snat2*), glucose transporter type 1 (*Glut1*), insulin-like growth factor 2

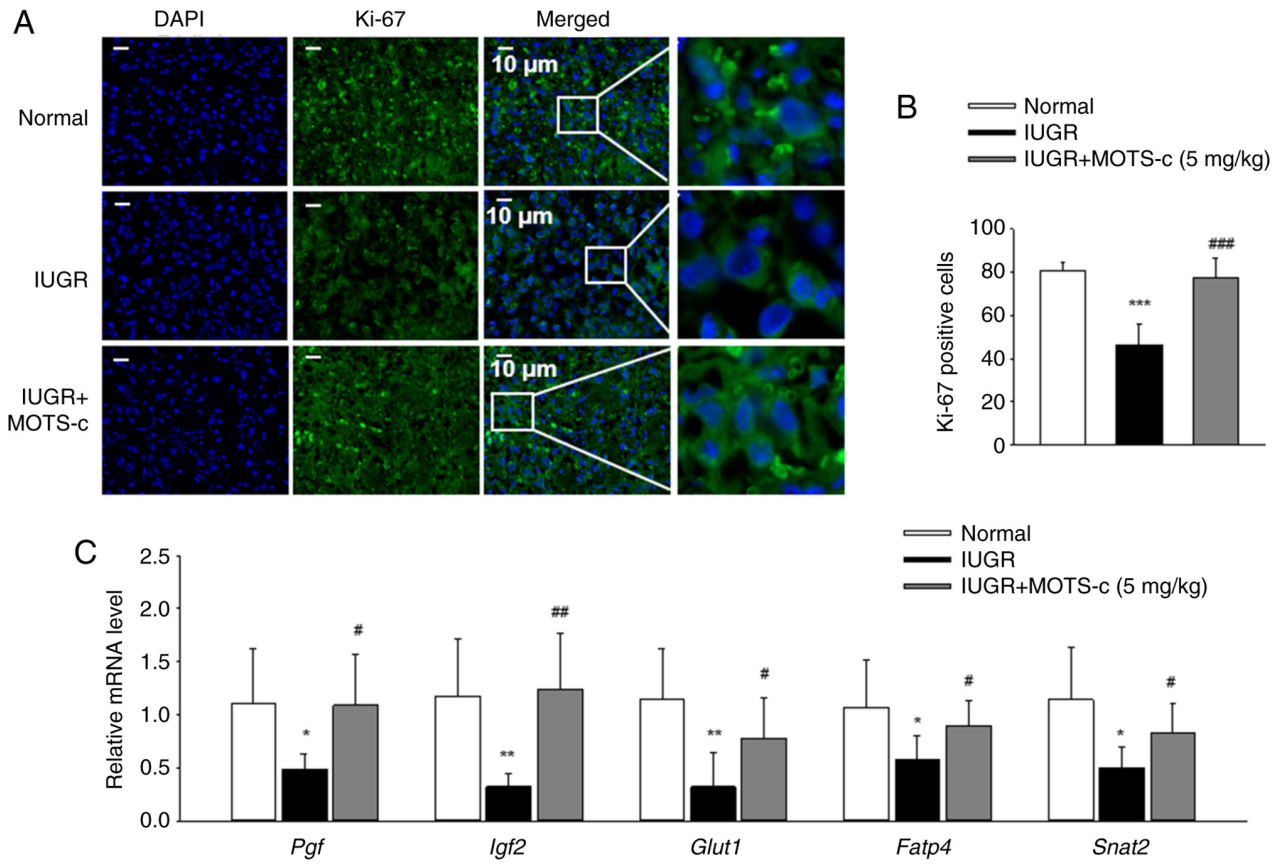

Figure 3. Administration of MOTS-c improves placental injury. (A) Representative immunofluorescence images of Ki-67 in placental tissues. Scale bar, 10 μm. (B) Qualification of Ki-67 positive cells. (C) Relative mRNA expression levels of *Pgf*, *Igf2*, *Glut1*, *Fatp4* and *Snat2* in placenta. Data are expressed as the mean ± SD. Normal, n=6; IUGR, n=6; IUGR + MOTS-c, n=5. *P<0.05 vs. normal, **P<0.01 vs. normal, ***P<0.001 vs. normal; $^{\#}$P<0.05 vs. IUGR; $^{\#\#}$P<0.01 vs. IUGR; $^{\#\#\#}$P<0.001 vs. IUGR. IUGR, intrauterine growth restriction; Pgf, placental growth factor; Igf2, insulin-like growth factor 2; Glut1, glucose transporter type 1; Fatp4, fatty acid transporter 4; Snat2, sodium-dependent neutral amino acid transporter-2.

(*Igf2*) and fatty acid transporter 4 (*Fatp4*) in placental tissues were assessed. Hypoxia exposure resulted in the downregulation of placental growth factors (*Pgf* and *Igf2*), as well as placental nutrient transport-related genes (*Glut1*, *Fatp4* and *Snat2*) in the IUGR group; MOTS-c treatment in the IUGR + MOTS-c group significantly increased the mRNA expression levels when compared with that in the IUGR group (Fig. 3C). These findings suggested that MOTS-c treatment exerted a beneficial effect on placental proliferation defects in hypoxic environments.

MOTS-c mitigates hypoxia-mediated oxidative stress in the placenta tissue. MOTS-c administration effectively mitigated oxidative stress-induced damage in placental tissues, as evidenced by a significant reduction in MDA levels and an increased SOD activity in the IUGR + MOTS-c group compared with that of the IUGR group (Fig. 4A and B). Nrf2, which upregulates the expressions of numerous antioxidant genes, serves a key role in inhibiting oxidative stress in the placenta (42). Maternal hypoxia exposure resulted in significantly decreased Nrf2 mRNA expression levels in the placenta of the IUGR group, while MOTS-c treatment restored Nrf2 mRNA expression levels in the IUGR + MOTS-c group (Fig. 4C). Furthermore, total, nuclear and cytoplasmic Nrf2 protein expression levels were also examined. Hypoxia restricted Nrf2 nuclear translocation, while MOTS-c significantly increased nuclear Nrf2 expression in placental tissues (Fig. 4D-G). The accumulation and nuclear translocation of Nrf2 was also detected by immunofluorescence, which demonstrated that in the IUGR + MOTS-c group, MOTS-c treatment promoted Nrf2 nuclear translocation compared with that in the IUGR group (Fig. 4H and I). In addition, MOTS-c treatment was associated with increased mRNA expression levels of heme oxygenase 1 and NAD(P)H quinone dehydrogenase 1, which are known Nrf2 downstream targeted anti-oxidative genes (Fig. 4J). These results suggest that MOTS-c activate Nrf2-mediated antioxidant pathway.

MOTS-c treatment attenuates hypoxia-induced injury in HUVEC cells. To elucidate the effects of MOTS-c on HUVECs, MOTS-c (10 μM) was used for subsequent *in vitro* assays, according to the CCK-8 results (Fig. S4A), since MOTS-c (20 and 40 μM) resulted in significantly decreased cell viability. It was demonstrated that MOTS-c content significantly decreased after hypoxic stimuli compared with HUVECs in normoxic conditions, which was consistent with the *in vivo* results. Exogenous MOTS-c (10 μM) significantly increased the MOTS-c content in hypoxia-induced HUVECs compared with that in the hypoxia group. (Fig. 5A). MOTS-c administration restored hypoxia-induced abnormal morphology in HUVECs (Fig. 5B) and significantly increased tube formation of HUVECs (Fig. 5C and D) compared with that in the

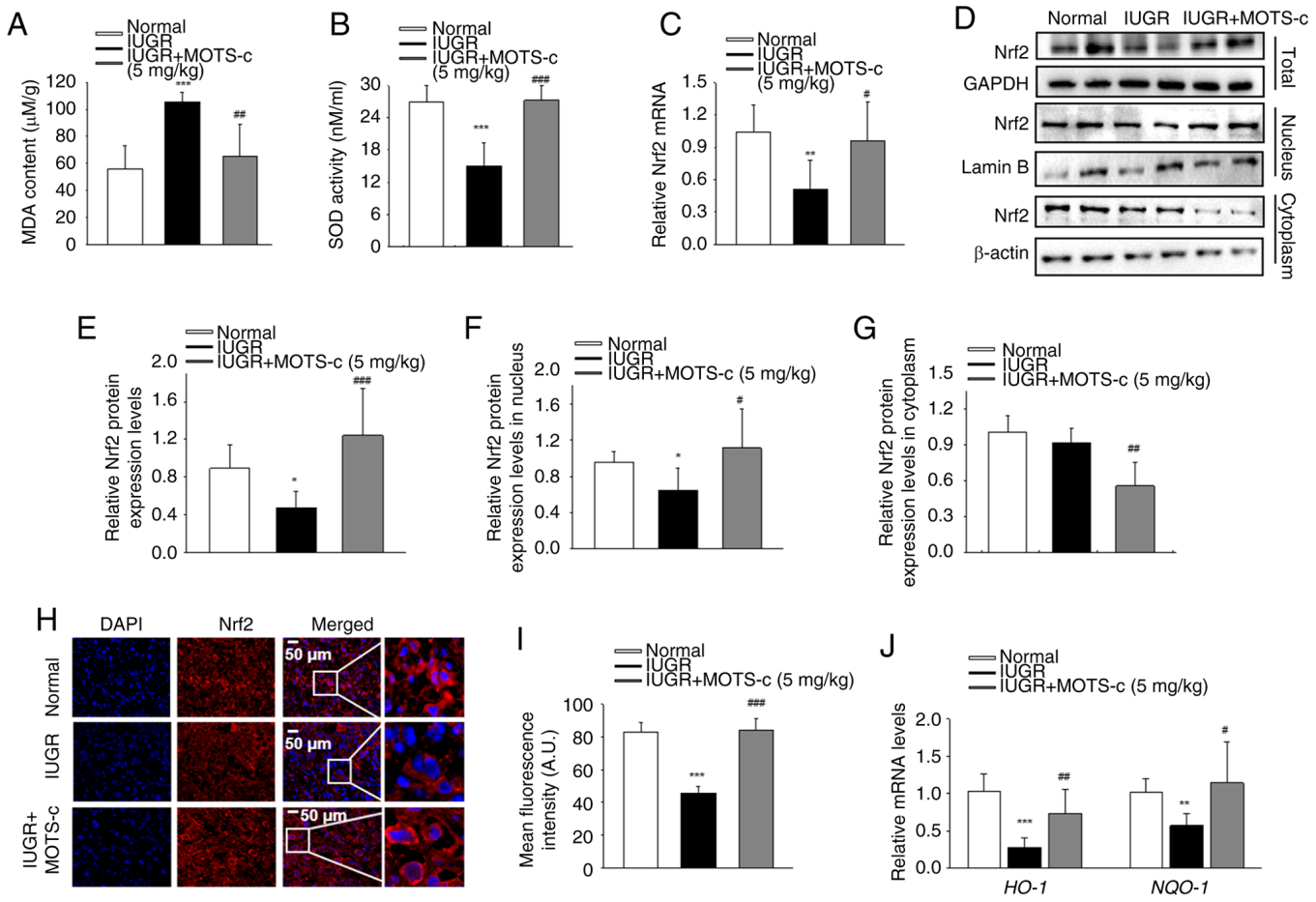

Figure 4. MOTS-c mitigates hypoxia-mediated oxidative stress in placenta. (A) MDA content in placenta. (B) SOD activity in placenta. (C) Nrf2 mRNA expression levels in placenta. (D) Representative western blotting images. (E) Total Nrf2 expression in placental tissues. (F) Nuclear Nrf2 expression in placental tissues. (G) Nrf2 expression in cytoplasm of placental tissues. (H) Representative immunofluorescence images and (I) quantification of Nrf2 in placenta. Scale bar, 50 μm. (J) Relative mRNA expression levels of HO-1 and NQO-1. Data are expressed as the mean ± SD. Normal, n=6; IUGR, n=6; IUGR + MOTS-c, n=5. *P<0.05 vs. normal, **P<0.01 vs. normal, ***P<0.001 vs. normal; $^{\#}$P<0.05 vs. IUGR; $^{\#\#}$P<0.01 vs. IUGR; $^{\#\#\#}$P<0.001 vs. IUGR. IUGR, intrauterine growth restriction; SOD, superoxide dismutase; MDA, malondialdehyde; Nrf2, nuclear factor erythroid 2-related factor 2; HO-1, heme oxygenase 1; NQO-1, NAD(P)H quinone dehydrogenase 1.

hypoxia group. Furthermore, MOTS-c treatment increased mRNA expression levels of *CD31*, *VEGFA* and *VEGFR2* under hypoxic conditions in HUVECs compared with that in the hypoxia group (Fig. 5E). In addition, MOTS-c treatment promoted proliferation in hypoxia-exposed HUVECs, as evidenced by the significantly increased levels of Ki-67 positive cells under MOTS-c treatment compared with the control group (Fig. S4B and C). These results suggested that MOTS-c mitigated hypoxia-induced injury and promoted angiogenesis and proliferation in HUVECs.

It was further investigated whether MOTS-c functions in other cell types in the placenta; placental trophoblast cells are critically important for pregnancy and embryonic development (43). Thus, human placental trophoblast cells (HTR-8/SVneo) was also examined. MOTS-c treatment significantly increased cell viability reduced cell injury and enhanced the mRNA levels of nutrient transporter genes, including *Pgf*, *Igf2*, *Glut1*, *Fatp4* and *Snat2* (Fig. S5A-C). Furthermore, MOTS-c treatment significantly reduced ROS production in hypoxia-stimulated HTR-8/SVneo cells compared with that of the PBS treated HTR-8/SVneo cells under hypoxic conditions (Fig. S5D and E). These results indicated that the beneficial effects of MOTS-c against hypoxia was not limited to HUVECs.

MOTS-c treatment increased Nrf2 nuclear translocation and attenuated mitochondrial injury in HUVECs. The antioxidant effect of MOTS-c treatment was also examined in HUVECs. Intracellular ROS production was assessed using DCFH-DA staining, which demonstrated that MOTS-c treatment significantly suppressed the hypoxia-induced ROS generation compared with that of PBS-treated hypoxic cells (Fig. 6A). Furthermore, MOTS-c treatment under hypoxic conditions resulted in significantly reduced MDA content and restored SOD activity in HUVECs compared with that of PBS-treated hypoxic cells (Fig. 6B and C). Additionally, mitochondrial ROS levels were evaluated using MitoSOX staining, which similarly demonstrated that MOTS-c treatment significantly inhibited hypoxia-induced mitochondrial ROS generation compared with that of PBS-treated hypoxic cells (Fig. 6D). Concurrently, MMP levels was assessed using JC-1 staining, which demonstrated that MOTS-c significantly reduced MMP levels in hypoxic HUVECs compared with untreated cells (Fig. 6E). Consistent with the present *in vivo* findings,

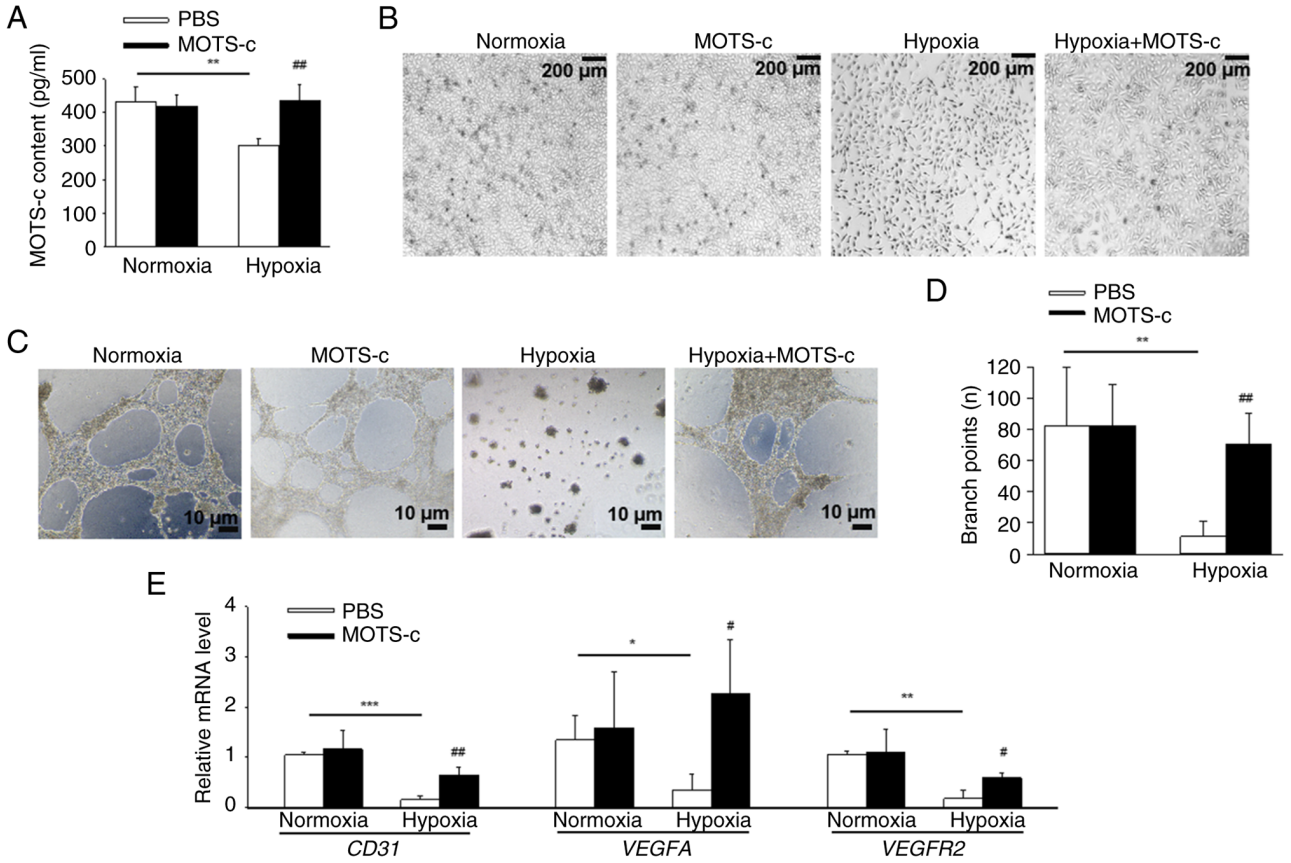

Figure 5. MOTS-c exposure promotes angiogenesis in HUVECs. (A) MOTS-c content in HUVECs. (B) Cell morphology under white light. Scale bar, 200 μm. (C) Representative images and (D) quantitative analysis of the *in vitro* tube formation. Scale bar, 10 μm. (E) Relative mRNA expression levels of *CD31*, *VEGFA* and *VEGFR2* in HUVECs. Results are representative of three independent experiments. Data are expressed as mean ± SD, n=4. *P<0.05, **P<0.01, ***P<0.001; $^{\#}$P<0.05 vs. PBS under hypoxic conditions, $^{\#\#}$P<0.01 vs. PBS under hypoxic conditions. VEGFA, vascular endothelial growth factor A; VEGFR2, VEGF receptor 2.

MOTS-c treatment promoted Nrf2 nuclear translocation in hypoxia-induced HUVECs (Fig. 6F and G). These findings suggested that MOTS-c exerted its protective effects, at least in part, through enhanced Nrf2 activity and by mitigating mitochondrial injury in hypoxia-induced HUVECs.

Nrf2 inhibitor ML385 offsets the protective effect of MOTS-c against hypoxia in HUVECs. To investigate whether Nrf2 serves a role in the protective effects of MOTS-c against hypoxia in HUVECs, ML385, a specific Nrf2 inhibitor was used (39). It was demonstrated that pretreatment with ML385 under hypoxic conditions inhibited tube formation compared with the hypoxia group, implying the significance of Nrf2. MOTS-c treatment, upon co-administration of ML385 in hypoxia-induced HUVECs, failed to promote tube formation (Fig. 7A and B). Additionally, pretreatment with ML385 under hypoxic conditions increased ROS production compared with the hypoxia group, and MOTS-c did not reduce the generation of ROS in ML385-pretreated HUVECs under hypoxic stimuli (Fig. 7C and D). These findings suggested that the protective effect of MOTS-c against hypoxia-induced HUVECs injury in HUVECs may partially rely on Nrf2 activation.

Nrf2 overexpression fails to enhance the beneficial effect of MOTS-c on hypoxia-stimulated HUVECs. In addition to Nrf2 inhibition, the effects of Nrf2 overexpression on hypoxia-exposed HUVECs was also determined. Under hypoxic conditions, Nrf2 overexpression significantly increased Nrf2 mRNA expression levels in HUVECs compared with control cells, which indicated the efficiency of the Nrf2 transfection (Fig. 8A). Nrf2 overexpression significantly enhanced cell viability under hypoxic conditions. However, there was no significant difference between the Nrf OE and MOTS-c + Nrf2 OE groups under hypoxic stimuli (Fig. 8B). In addition, Nrf2 overexpression markedly reduced ROS production under hypoxic conditions, and Nrf2 overexpression failed to further inhibit ROS generation in MOTS-c treated HUVECs under hypoxic conditions (Fig. 8C and D).

MOTS-c protects against hypoxia-induced placental insufficiency in an Nrf2-dependent manner. To further investigate the role of Nrf2 in the protective effects of MOTS-c against hypoxia-induced IUGR and placental insufficiency, $Nrf2^{-/-}$ pregnant mice were exposed to hypoxic conditions for further investigation. Placental tissues from $Nrf2^{-/-}$ mice exhibited no Nrf2 protein expression (Fig. S6A and B). MOTS-c treatment did not affect fetal growth restriction in Nrf2 deficiency mice, as evidenced by unchanged fetal size, morphology and the fetal to placenta weight ratio in $Nrf2^{-/-}$ pregnant mice when compared with the hypoxia-treated $Nrf2^{-/-}$ pregnant mice (Fig. 9A and B). Notably, MOTS-c administration failed to enhance the blood sinus areas (Fig. 9C and D) and did not upregulate the protein expressions of CD31, VEGFA and

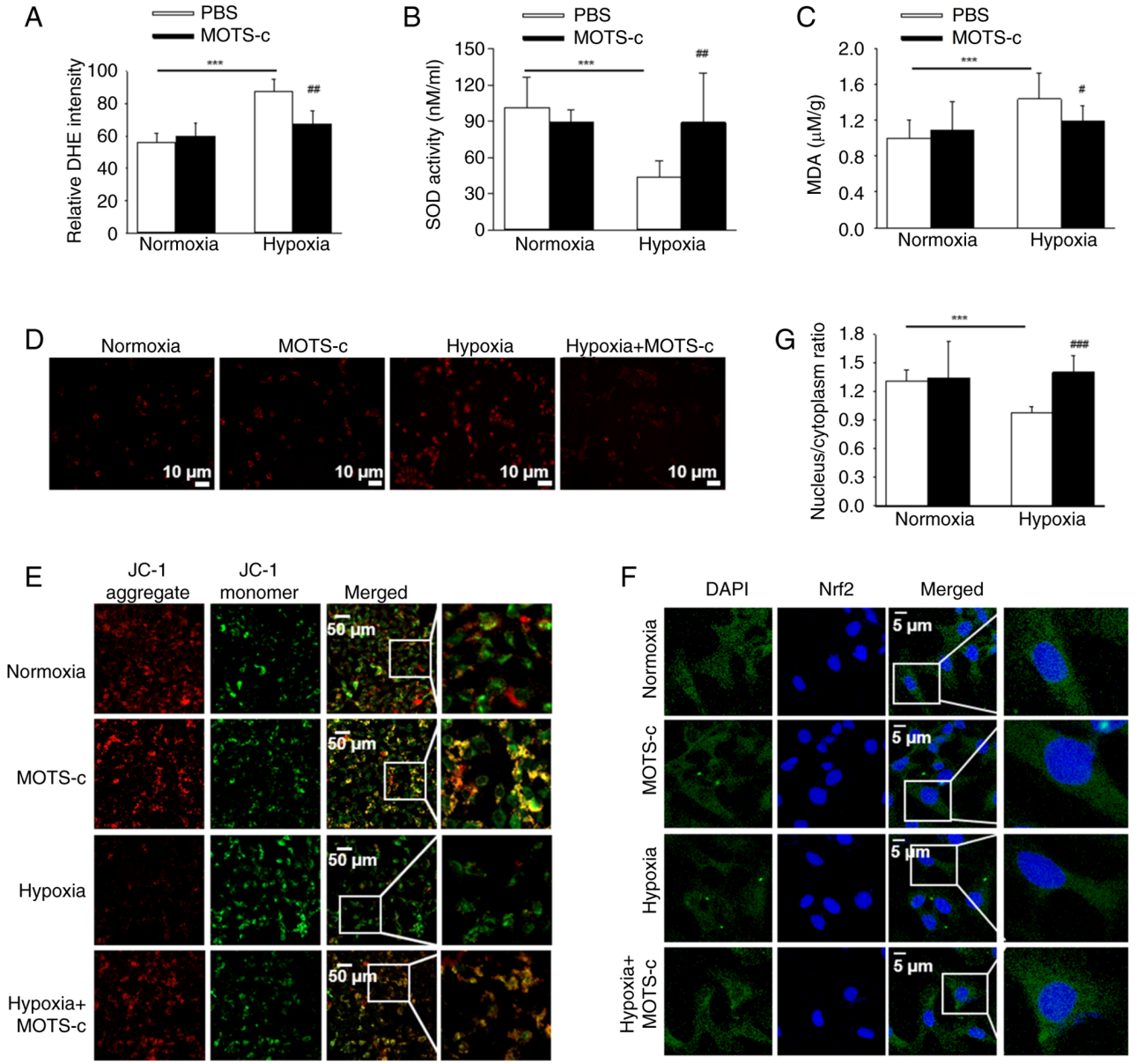

Figure 6. MOTS-c exposure attenuates oxidative stress in HUVECs. (A) Relative intensity of DCFH-DA staining. (B) Cellular SOD activity. (C) Cellular MDA content. (D) Representative images of MitoSOX staining. Scale bar, 10 μm. (E) Representative images of JC-1 staining. Scale bar, 50 μm. (F) Representative immunofluorescence images of Nrf2 in HUVECs. Scale bar, 5 μm. (G) Relative nuclear to cytoplasm fluorescence ratio. Results are representative of three independent experiments. Data are expressed as the mean ± SD, n=4. ***P<0.001, $^{\#}$P<0.05 vs. PBS under hypoxic conditions, $^{\#\#}$P<0.01 vs. PBS under hypoxic conditions; $^{\#\#\#}$P<0.001 vs. PBS under hypoxic conditions. SOD, superoxide dismutase; MDA, malondialdehyde; DCFH-DA,2'7'-dichlorodihydro fluorescein diacetate ; Nrf2, nuclear factor erythroid 2-related factor 2.

VEGFR2 in Nrf2$^{-/-}$ mice (Fig. 9E). Additionally, MOTS-c supplementation did not impact the mRNA expressions of placental growth factors, including *Pgf* and *Igf2* in Nrf2$^{-/-}$ mice. However, MOTS-c upregulated the expression levels of placental nutrient transport-related genes, such as *Glut1*, *Fatp4* and *Snat2*, in Nrf2$^{-/-}$ mice (Fig. 9F). This suggested that the beneficial effects of MOTS-c on placental nutrient transport-related genes might be independent of Nrf2.

Discussion

IUGR is characterized by a fetus that is small for gestational age. A study of 600,000 stillbirths (≥22 weeks) from 12 countries reported that being small for gestational age contributed to ~20% of term stillbirths (2). However, there is currently no effective treatment for IUGR. The present study investigated the effects of MOTS-c peptides on hypoxia-induced IUGR, and demonstrated that MOTS-c administration significantly mitigated hypoxia-induced IUGR, promoted placental angiogenesis, suppressed oxidative stress and ameliorated placental injury both *in vivo* and *in vitro*. Furthermore, the protective effects of MOTS-c were shown to be Nrf2-dependent, as the protective effect of MOTS-c were abolished not only in Nrf2 inhibitor treated HUVECs, but also in Nrf2 KO mice. To the best of our knowledge, the present study is the first to demonstrate that MOTS-c treatment could attenuate hypoxia-induced IUGR, and thus suggest a new strategy for treating hypoxia-related neonatal disease.

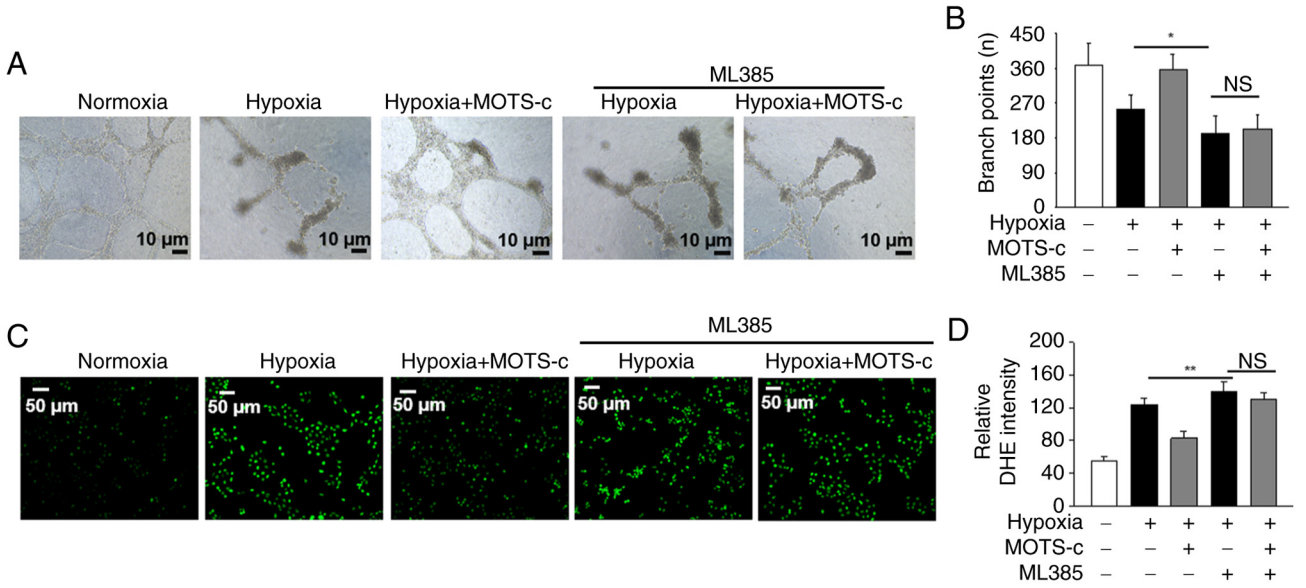

Figure 7. Nrf2 inhibitor ML385 offset the protective effect of MOTS-c against hypoxia-induced dysregulated angiogenesis and oxidative stress in HUVECs. (A) Representative images and (B) quantitative analysis of the *in vitro* tube formation. Scale bar, 10 μm. (C) Representative images of DCFH-DA staining and (D) quantification of cellular ROS. Scale bar, 50 μm. Results are representative of three independent experiments. Data are expressed as the mean ± SD. *P<0.05, **P<0.01. NS, not significant; DCFH-DA,2',7'-dichlorodihydro fluorescein diacetate; Nrf2, nuclear factor erythroid 2-related factor 2.

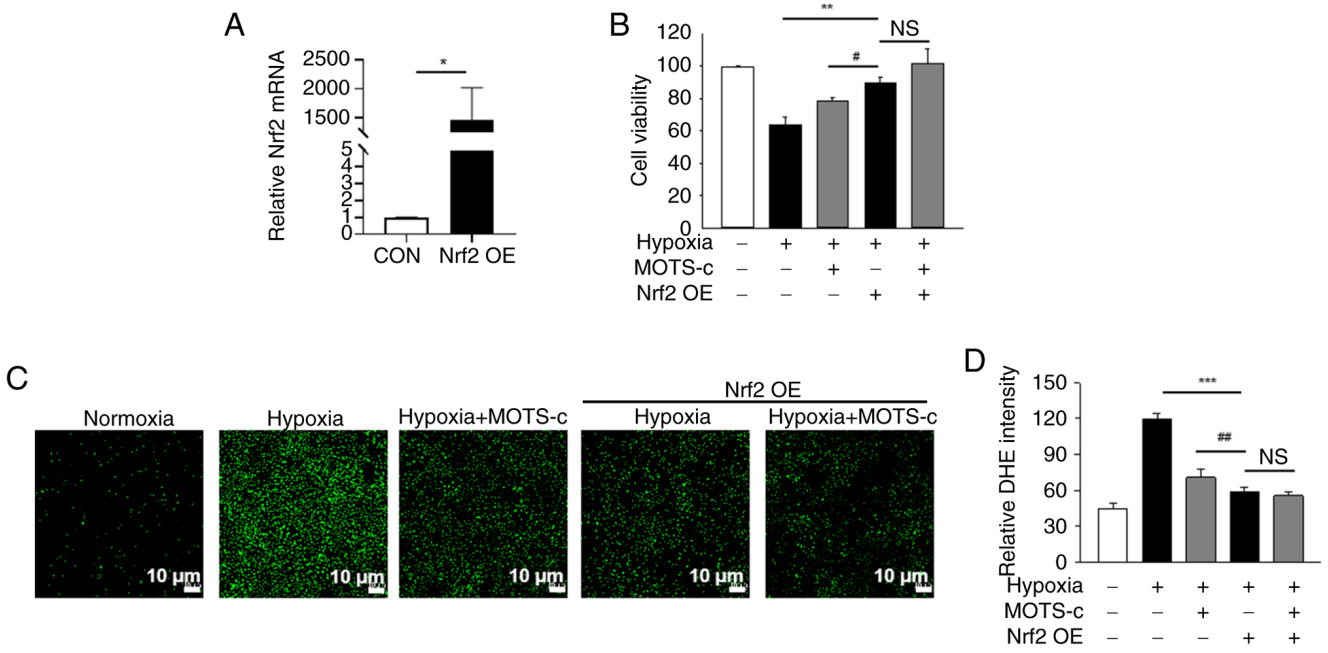

Figure 8. Nrf2 overexpression does not enhance the beneficial effects of MOTS-c on hypoxia-stimulated HUVECs. (A) Relative Nrf2 mRNA expression levels. (B) Cell viability. (C). Representative images of DCFH-DA staining and (D) quantification of cellular ROS. Scale bar, 10 μm. Data are expressed as the mean ± SD. *P<0.05, **P<0.01, ***P<0.001, $^{\#}$P<0.05, $^{\#\#}$P<0.01. NS, not significant; Nrf2, nuclear factor erythroid 2-related factor 2; ROS, reactive oxygen species; OE, overexpression; DCFH-DA, 2',7'-dichlorodihydro fluorescein diacetate.

Prenatal hypoxia, a common consequence of complicated pregnancies, serves a key role in triggering IUGR (44,45). In such cases, the placenta fails to adequately supply oxygen and nutrients to the developing fetus, resulting in low birth weight (LBW) (7). Normal development of the placental vascular tree is essential for both proper placental growth and nutrient delivery from mother to fetus. Studies have reported impaired angiogenesis in placental tissues of infants with LBW (46,47), which has been identified as an important pathophysiologic contributor to IUGR. VEGFA and its receptor VEGFR2 are vital for blood vessel development and their reduction has been observed in LBW placentas (48). Higher expression of the NADPH oxidase 2 and lower vessel density were found in LBW placentas, as NADPH oxidase 2 inhibited VEGFA-mediated placental angiogenesis (49). Dietary supplementation with adenosine has been shown to enhance placental angiogenesis and reduce the incidence of IUGR in piglets (50). Therefore, improving placental angiogenesis appears crucial for

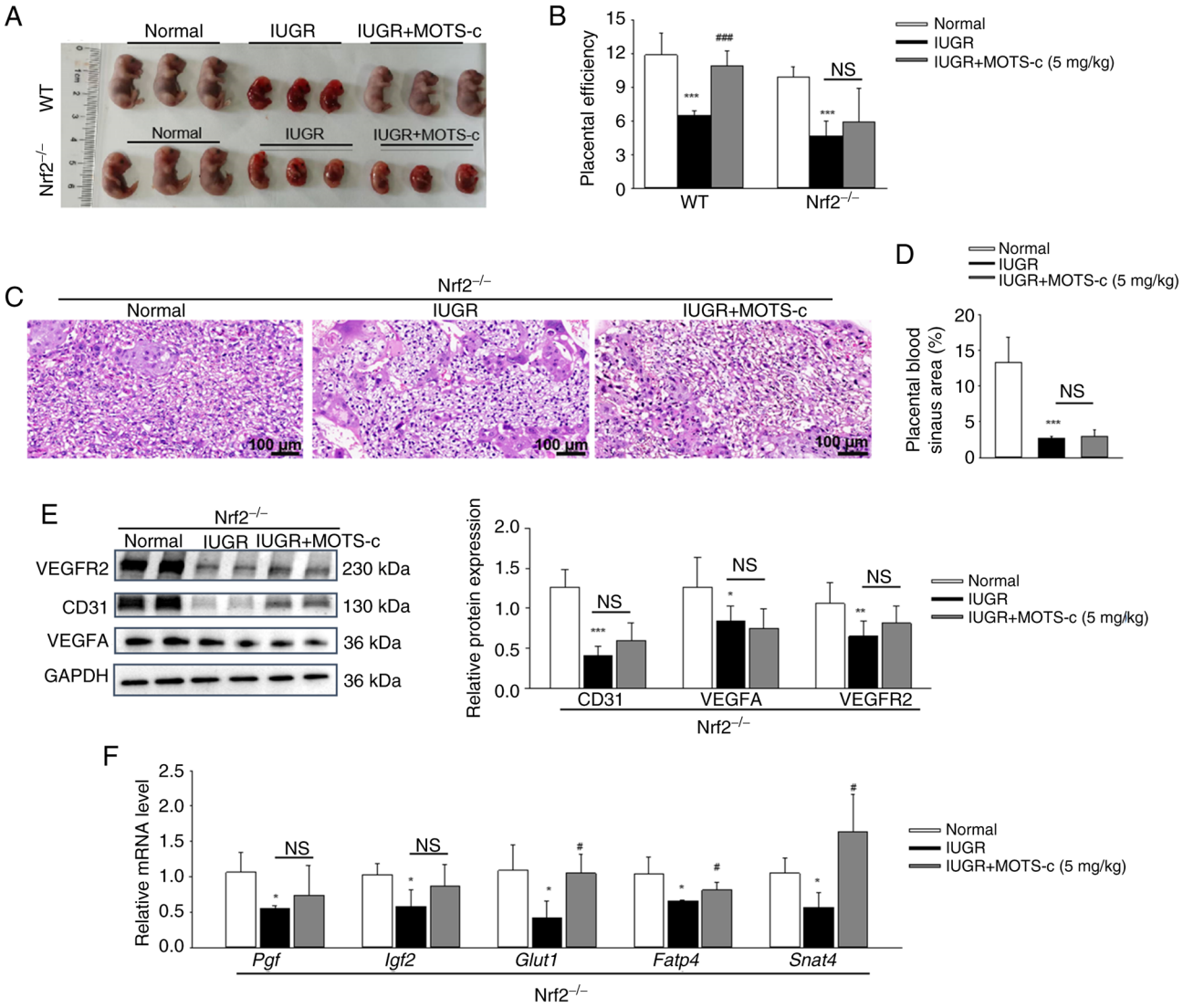

Figure 9. MOTS-c protects against hypoxia-induced placental insufficiency in an Nrf2-dependent manner. (A) Morphology of fetal mice on GD17.5 in WT and Nrf2 KO mice. (B) Placental efficiency, which represents the ratio of fetal to placenta weight. (C) Representative images of H&E staining of placental tissues. Scale bar, 100 μm. (D) Quantification of the placental blood sinus area. (E) Western blotting analysis of CD31, VEGFA and VEGFR2 protein expression levels in placenta. (F) Relative mRNA expression levels of *Pgf*, *Igf2*, *Glut1*, *Fatp4* and *Snat2* in placenta. Data are expressed as mean ± SD. n=4-6. *P<0.05 vs. normal, **P<0.01 vs. normal, ***P<0.001 vs. normal, $^{\#}$P<0.05 vs. IUGR, $^{\#\#\#}$P<0.001 vs. IUGR.. NS, not significant; IUGR, intrauterine growth restriction; GD, gestational day; Pgf, placental growth factor; Nrf2, nuclear factor erythroid 2-related factor 2; Igf2, insulin-like growth factor 2; Glut1, glucose transporter type 1; Fatp4, fatty acid transporter 4; Snat2, sodium-dependent neutral amino acid transporter-2; VEGFA, vascular endothelial growth factor A; VEGFR2, VEGF receptor 2.

alleviating IUGR. Consistent with this notion, the present study demonstrated that MOTS-c treatment accelerated the formation of placental blood vessels in IUGR by increasing blood sinus areas and upregulating angiogenesis-related markers CD31 and VEGF. In addition, increased Ki-67 positive cells in both placental tissues and hypoxia-exposed HUVECs were observed. Ki-67 is widely considered a marker of proliferation, which is mainly expressed during the active phases of the cell cycle: G_1, S, G_2 and mitosis (51). However, low amounts of Ki-67 may also be detected in quiescent cells (52). The present study found positive Ki-67 signals peripheral to DAPI staining in placental tissues, while the Ki-67 signal was totally located in the nucleus of HUVECs. The observed extra-nuclear Ki-67 immunofluorescence signal in tissues is a well-documented phenomenon as reported in previous studies (53,54). It was considered that the apparent peripheral signal potentially reflected different cell type and cell cycle stages. Furthermore, MOTS-c was injected intraperitoneally from GD 11 to 17.5, and beneficial effects of MOTS-c administration on maintaining placenta angiogenesis and proliferation, attenuating placental insufficiency, and subsequently alleviating IUGR were observed. The timing of the experiment was aligned with prior work, in which MOTS-c was administered concurrently with the induction of the disease model (10,30,31,55).

The placenta is highly susceptible to oxidative stress, which in turn triggers placental vascular dysfunction and insufficiency (56). Oxidative stress in the placenta is a major contributor to the development of IUGR. Elevated levels of MDA and decreased catalase activity have been observed in plasma and placental tissues of pregnancies with IUGR (57). Therefore, restoring redox homeostasis through antioxidant therapy would be an effective treatment for these pregnancy complications (58). However, a previous clinical trial showed limited success in using antioxidant therapy for hypoxic

pregnancy (59,60). Therefore, further investigation into alternative treatment options for IUGR is warranted. The present study found that that administration of MOTS-c reduced MDA content and increased SOD activity in placental tissues. The *in vitro* experiments demonstrated a decrease in ROS generation after MOTS-c treatment in hypoxia-induced HUVECs, which indicated the anti-oxidative stress effects of MOTS-c. Dysfunctional mitochondria are another source of ROS overproduction in individuals with IUGR (61). The present study demonstrated that MOTS-c treatment reduced MMP levels and inhibited mitochondria ROS generation, which suggested a protective role of MOTS-c on mitochondrial function. These results indicated that MOTS-c ameliorated mitochondrial dysfunction and restored antioxidant enzymes, thereby reducing ROS generation and alleviated placental insufficiency in IUGR.

The transcription factor Nrf2 serves a crucial role in coordinating the cellular antioxidant defense system, regulating the expression of >100 genes involved in oxidative stress responses and detoxification processes (62,63). The activation of Nrf2 is suggested to be a compensatory mechanism that safeguards the fetus against oxidative damage. A previous study reported that in both human and rat IUGR groups, placentas had lower Nrf2 expression levels compared with that of the control group placentas (64). Similarly, the downregulation of Nrf2 was found in placental tissues from patients with eclampsia (65). The present study similarly demonstrated downregulated expression of Nrf2, especially the reduced nuclear Nrf2 expression in hypoxia-induced maternal placenta compared with the normal group of mice, and that MOTS-c administration increased Nrf2 nuclear accumulation compared with the IUGR group. Cytoplasmic and nuclear Nrf2 protein expressions were verified through immunoblotting, and Nrf2 immunofluorescence was performed. However, there remains a limitation regarding the quantitative analyses of Nrf2 distribution (nuclear/cytoplasmic ratio) in placenta tissue in the present study. The detection of Nrf2 subcellular localization is important as nuclear translocation of Nrf2 directly reflect its activation status (19), thus further research regarding Nrf2 subcellular localization, particularly precise quantification is warranted. Additionally, increased transcriptional activity of Nrf2 under MOTS-c administration was demonstrated in the present study. However, it was assessed at only one time point, and the relevant pharmacokinetics of Nrf2 activation over time following MOTS-c administration is important to optimize dosing regimen to maintain efficacy of MOTS-c. For example, to investigate the optimal Nrf2 activity time after MOTS-c treatment, future work could establish the Nrf2 signaling pathway activation reporting system using secreted Gaussia luciferase (Gluc) as the reporter gene, thus the activity of Gluc could be monitored constantly in MOTS-c-treated cells. Furthermore, a reporter protein complementation imaging assay could be established to screen and observe Nrf2 nuclear translocation in MOTS-c-treated cells and living animals in the future.

The protective effects of MOTS-c were abolished when the Nrf2 inhibitor ML385 and Nrf2 KO mice were used in the present study. By contrast, Nrf2 overexpression failed to enhance the beneficial effects of MOTS-c on cell viability and ROS generation in hypoxia-stimulated HUVECs, in which there was no difference between the Hypoxia + Nrf2 OE and Hypoxia + MOTS-c + Nrf2 OE groups. Notably, under hypoxic conditions, Nrf2 overexpression (Hypoxia + Nrf2 OE group) demonstrated more pronounced cytoprotective effects (increased cell viability and decreased ROS production) compared with that of MOTS-c-treated cells (Hypoxia + MOTS-c group). This result further highlighted the central regulatory role of Nrf2 against oxidative stress damage, which overall suggested that the protective role of MOTS-c against hypoxia-induced abnormal placental injury and fetal growth is at least partially dependent on Nrf2. However, the specific mechanism how MOTS-c regulates Nrf2 has not been fully elucidated until now. Previous studies from the present research group have demonstrated that MOTS-c could directly increase synthesis of Nrf2 independent of protein degradation and promote Nrf2 nuclear translocation (21,22), and demonstrated nuclear accumulation of Nrf2 under MOTS-c administration in the IUGR model. Future research should focus on elucidating the regulatory mechanism of MOTS-c on Nrf2 and investigating the impact of MOTS-c presence or absence on the interaction between Nrf2 and KEAP1 in response to hypoxia or other stress conditions. Notably, the mRNA expression levels of nutrient transporters (*Glut1*, *Fatp4* and *Snat4*) were still upregulated under MOTS-c administration in Nrf2 KO mice in the present study. It has been reported that MOTS-c induces glucose uptake and GLUT4 translocation in mitochondrial fusion dependent way, and that MOTS-c functionally prevents nutrient metabolism disorders, including insulin resistance, obesity and bone metabolism (66). These studies suggest that MOTS-c can function on nutrient transporters in other non-Nrf2-dependent pathways, such as targeting the mitochondrion. Our previous study found altered glucose and lipid metabolic levels in IUGR offspring *in vivo* (28); whether MOTS-c treatment alters actual amino acid, glucose or fatty acid levels in fetal serum and functions in regulating glucose or fatty acid in the offspring could be investigated in future research.

The present study has several clinical implications. First, significantly decreased maternal serum MOTS-c content following hypoxic exposure was observed, which suggested that plasma MOTS content could potentially serve as a novel marker for diagnosing IUGR. Second, the *in vivo* and *in vitro* experiments demonstrated that administration of MOTS-c effectively attenuated hypoxia-induced IUGR, which suggested that MOTS-c peptides may offer a novel therapeutic approach for treating hypoxia-related neonatal disease, including IUGR.

Several limitations of the present study should be acknowledged. First, a single dose of MOTS-c (5 mg/kg) was used in the present study from GD11 to GD17.5; however, future work should include a dose-response experiment from GD11 to GD17.5 or at later stages in pregnancy to determine the optimal therapeutic concentration, administration time and potential toxicity of MOTS-c. Second, further randomized clinical trials are needed to confirm the endogenous levels of MOTS-c in human placentas or maternal serum from IUGR pregnancies to further the clinical understanding of MOTS-c in IUGR. Currently, the MOTS-c ELISA kit is most commonly used to determine MOTS-c content in body fluids, such as serum. However, this detection system present challenges and can potentially lead to strongly differing results (67). The previous study has established an LC/MS-based method for

MOTS-c quantification; therefore, serum or amniotic fluid MOTS-c content may be measured in human IUGR pregnancies using LC/MS in future (67). Furthermore, future studies should focus on the long-term development of main organs such as lungs, heart and brain in offspring mice following MOTS-c administration in an IUGR mouse model.

In conclusion, MOTS-c treatment effectively improved placental insufficiency in hypoxia-induced IUGR by activating the Nrf2-mediated anti-oxidant pathway. The present provided insights for developing MOTS-c as a therapeutic strategy for fetal diseases associated with hypoxic pregnancy, including IUGR.

Acknowledgements

Not applicable.

Funding

The present study was supported by the National Natural Science Foundation of China (grant nos. 82171704 and 82100018), Natural Science Foundation of Jiangsu Province (grant no. BE2023684), Natural Science Foundation of Shandong Province (grant no. ZR2021MH333), Fundamental Research Funds for the Central Universities (grant no. JUSRP121062), Translational medicine Project of Wuxi Commission of Health (grant no. ZH202101), Wuxi Taihu Talent Training Project (Double hundred Medical Youth Professionals Program; grant no. HB2020054) and the clinical research and translational medicine program of the Affiliated Hospital of Jiangnan University (grant no. LCYJ202239).

Availability of data and materials

The data generated in the present study may be requested from the corresponding author.

Authors' contributions

DC, HMZ and QFP performed study conceptualization. HMZ and XLS managed project administration and data collection. SPL, SCL and ZXX conducted investigation, provided resources, developed software and performed validation. YXW and JFH curated data. DC, XLS, YXW, JFH and QFP acquired funding. DC, QFP and JFH contributed to writing. DC and HMZ confirm the authenticity of all the raw data. All authors read and approved the final manuscript.

Ethics approval and consent to participate

The experimental procedures were approved by the Experimental Animal Care and Use Committee of Jiangnan University [approval nos. 20220930m1080501(383) and 20231115m1080530(555)] and conducted according to the Guide for the Care and Use of Laboratory Animal published by the US National Institutes of Health (8th edition).

Patient consent for publication

Not applicable.

Competing interests

The authors declare that they have no competing interests.

References

1. Ahmadzadeh E, Polglase GR, Stojanovska V, Herlenius E, Walker DW, Miller SL and Allison BJ: Does fetal growth restriction induce neuropathology within the developing brainstem? J Physiol 601: 4667-4689, 2023.
2. Lawn JE, Ohuma EO, Bradley E, Idueta LS, Hazel E, Okwaraji YB, Erchick DJ, Yargawa J, Katz J, Lee ACC, *et al*: Small babies, big risks: Global estimates of prevalence and mortality for vulnerable newborns to accelerate change and improve counting. Lancet 401: 1707-1719, 2023.
3. Jardine J, Walker K, Gurol-Urganci I, Webster K, Muller P, Hawdon J, Khalil A, Harris T, van der Meulen J; National Maternity and Perinatal Audit Project Team: Adverse pregnancy outcomes attributable to socioeconomic and ethnic inequalities in England: A national cohort study. Lancet 398: 1905-1912, 2021.
4. Reynolds LP, Borowicz PP, Caton JS, Crouse MS, Dahlen CR and Ward AK: Developmental programming of fetal growth and development. Vet Clin North Am Food Anim Pract 35: 229-247, 2019.
5. Hendrix MLE, Bons JA, Alers NO, Severens-Rijvers CAH, Spaanderman MEA and Al-Nasiry S: Maternal vascular malformation in the placenta is an indicator for fetal growth restriction irrespective of neonatal birthweight. Placenta 87: 8-15, 2019.
6. Zur RL, Kingdom JC, Parks WT and Hobson SR: The placental basis of fetal growth restriction. Obstet Gynecol Clin North Am 47: 81-98, 2020.
7. D'Agostin M, Di Sipio Morgia C, Vento G and Nobile S: Long-term implications of fetal growth restriction. World J Clin Cases 11: 2855-2863, 2023.
8. Perez M, Robbins ME, Revhaug C and Saugstad OD: Oxygen radical disease in the newborn, revisited: Oxidative stress and disease in the newborn period. Free Radic Biol Med 142: 61-72, 2019.
9. Joo EH, Kim YR, Kim N, Jung JE, Han SH and Cho HY: Effect of endogenic and exogenic oxidative stress triggers on adverse pregnancy outcomes: Preeclampsia, fetal growth restriction, gestational diabetes mellitus and preterm birth. Int J Mol Sci 22: 10122, 2021.
10. Lee C, Zeng J, Drew BG, Sallam T, Martin-Montalvo A, Wan J, Kim SJ, Mehta H, Hevener AL, de Cabo R and Cohen P: The mitochondrial-derived peptide MOTS-c promotes metabolic homeostasis and reduces obesity and insulin resistance. Cell Metab 21: 443-454, 2015.
11. Kim KH, Son JM, Benayoun BA and Lee C: The mitochondrial-encoded peptide MOTS-c translocates to the nucleus to regulate nuclear gene expression in response to metabolic stress. Cell Metab 28: 516-524.e7, 2018.
12. Shen C, Wang J, Feng M, Peng J, Du X, Chu H and Chen X: The mitochondrial-derived peptide MOTS-c attenuates oxidative stress injury and the inflammatory response of H9c2 cells through the Nrf2/ARE and NF-κB pathways. Cardiovasc Eng Technol 13: 651-661, 2022.
13. Xiao J, Zhang Q, Shan Y, Ye F, Zhang X, Cheng J, Wang X, Zhao Y, Dan G, Chen M and Sai Y: The mitochondrial-derived peptide (MOTS-c) interacted with Nrf2 to defend the antioxidant system to protect dopaminergic neurons against rotenone exposure. Mol Neurobiol 60: 5915-5930, 2023.
14. Kim SJ, Miller B, Kumagai H, Silverstein AR, Flores M and Yen K: Mitochondrial-derived peptides in aging and age-related diseases. Geroscience 43: 1113-1121, 2021.
15. Li Y, Li Z, Ren Y, Lei Y, Yang S, Shi Y, Peng H, Yang W, Guo T, Yu Y and Xiong Y: Mitochondrial-derived peptides in cardiovascular disease: Novel insights and therapeutic opportunities. J Adv Res 64: 99-115, 2024.
16. Wu N, Shen C, Wang J, Chen X and Zhong P: MOTS-c peptide attenuated diabetic cardiomyopathy in STZ-induced type 1 diabetic mouse model. Cardiovasc Drugs Ther 39: 491-498, 2025.
17. Yang M, Chen W, He L, Wang X, Liu D, Xiao L and Sun L: The role of mitokines in diabetic nephropathy. Curr Med Chem 32: 1276-1287, 2025.
18. Itoh K, Chiba T, Takahashi S, Ishii T, Igarashi K, Katoh Y, Oyake T, Hayashi N, Satoh K and Hatayama I: An Nrf2/small Maf heterodimer mediates the induction of phase II detoxifying enzyme genes through antioxidant response elements. Biochem Biophys Res Commun 236: 313-322, 1997.

19. Ulasov AV, Rosenkranz AA, Georgiev GP and Sobolev AS: Nrf2/Keap1/ARE signaling: Towards specific regulation. Life Sci 291: 120111, 2022.
20. Fasipe B, Li S and Laher I: Exercise and vascular function in sedentary lifestyles in humans. Pflugers Arch 475: 845-856, 2023.
21. Wang DD, Xu B, Sun JJ, Sui M, Li SP, Chen YJ, Zhang YL, Wu JB, Teng SY, Pang QF and Hu CX: MOTS-c mimics remote ischemic preconditioning in protecting against lung ischemia-reperfusion injury by alleviating endothelial barrier dysfunction. Free Radic Biol Med 229: 127-138, 2025.
22. Zhang Y, Huang J, Zhang Y, Jiang F, Li S, He S, Sun J, Chen D, Tong Y, Pang Q and Wu Y: The mitochondrial-derived peptide MOTS-c alleviates radiation pneumonitis via an Nrf2-dependent mechanism. Antioxidants (Basel) 13: 613, 2024.
23. Lamberto F, Peral-Sanchez I, Muenthaisong S, Zana M, Willaime-Morawek S and Dinnyés A: Environmental alterations during embryonic development: Studying the impact of stressors on pluripotent stem cell-derived cardiomyocytes. Genes (Basel) 12: 1564, 2021.
24. Kweider N, Huppertz B, Rath W, Lambertz J, Caspers R, ElMoursi M, Pecks U, Kadyrov M, Fragoulis A, Pufe T and Wruck CJ: The effects of Nrf2 deletion on placental morphology and exchange capacity in the mouse. J Matern Fetal Neonatal Med 30: 2068-2073, 2017.
25. The American Association for Accreditation of Laboratory Animal Care. JAMA 207: 1707, 1969.
26. Wang KCW, Larcombe AN, Berry LJ, Morton JS, Davidge ST, James AL and Noble PB: Foetal growth restriction in mice modifies postnatal airway responsiveness in an age and sex-dependent manner. Clin Sci (Lond) 132: 273-284, 2018.
27. Kalotas JO, Wang CJ, Noble PB and Wang KCW: Intrauterine growth restriction promotes postnatal airway hyperresponsiveness independent of allergic disease. Front Med (Lausanne) 8: 674324, 2021.
28. Chen D, Wang YY, Li SP, Zhao HM, Jiang FJ, Wu YX, Tong Y and Pang QF: Maternal propionate supplementation ameliorates glucose and lipid metabolic disturbance in hypoxia-induced fetal growth restriction. Food Funct 13: 10724-10736, 2022.
29. Chen D, Man LY, Wang YY, Zhu WY, Zhao HM, Li SP, Zhang YL, Li SC, Wu YX, Ling-Ai and Pang QF: Nrf2 deficiency exacerbated pulmonary pyroptosis in maternal hypoxia-induced intrauterine growth restriction offspring mice. Reprod Toxicol 129: 108671, 2024.
30. Lu H, Tang S, Xue C, Liu Y, Wang J, Zhang W, Luo W and Chen J: Mitochondrial-derived peptide MOTS-c increases adipose thermogenic activation to promote cold adaptation. Int J Mol Sci 20: 2456, 2019.
31. Tang M, Su Q, Duan Y, Fu Y, Liang M, Pan Y, Yuan J, Wang M, Pang X, Ma J, *et al*: The role of MOTS-c-mediated antioxidant defense in aerobic exercise alleviating diabetic myocardial injury. Sci Rep 13: 19781, 2023.
32. Li Z, LoBue A, Heuser SK, Li J, Engelhardt E, Papapetropoulos A, Patel HH, Lilley E, Ferdinandy P, Schulz R and Cortese-Krott MM: Best practices for blood collection and anaesthesia in mice: Selection, application and reporting. Br J Pharmacol 182: 2337-2353, 2025.
33. Mohamed AS, Hosney M, Bassiony H, Hassanein SS, Soliman AM, Fahmy SR and Gaafar K: Sodium pentobarbital dosages for exsanguination affect biochemical, molecular and histological measurements in rats. Sci Rep 10: 378, 2020.
34. Chen D, Qiu YB, Gao ZQ, Wu YX, Wan BB, Liu G, Chen JL, Zhou Q, Yu RQ and Pang QF: Sodium propionate attenuates the lipopolysaccharide-induced epithelial-mesenchymal transition via the PI3K/Akt/mTOR signaling pathway. J Agric Food Chem 68: 6554-6563, 2020.
35. Xia Y, Liu C, Li R, Zheng M, Feng B, Gao J, Long X, Li L, Li S, Zuo X and Li Y: Lactobacillus-derived indole-3-lactic acid ameliorates colitis in cesarean-born offspring via activation of aryl hydrocarbon receptor. iScience 26: 108279, 2023.
36. Chen Y, Wu Q, Wei J, Hu J and Zheng S: Effects of aspirin, vitamin D3, and progesterone on pregnancy outcomes in an autoimmune recurrent spontaneous abortion model. Braz J Med Biol Res 54: e9570, 2021.
37. Coin I, Beyermann M and Bienert M: Solid-phase peptide synthesis: From standard procedures to the synthesis of difficult sequences. Nat Protoc 2: 3247-3256, 2007.
38. Jia Y, Wang Q, Liang M and Huang K: KPNA2 promotes angiogenesis by regulating STAT3 phosphorylation. J Transl Med 20: 627, 2022.
39. Chen D, Gao ZQ, Wang YY, Wan BB, Liu G, Chen JL, Wu YX, Zhou Q, Jiang SY, Yu RQ, *et al*: Sodium propionate enhances Nrf2-mediated protective defense against oxidative stress and inflammation in lipopolysaccharide-induced neonatal mice. J Inflamm Res 14: 803-816, 2021.
40. Livak KJ and Schmittgen TD: Analysis of relative gene expression data using real-time quantitative PCR and the 2(-Delta Delta C(T)) method. Methods 25: 402-408, 2001.
41. Pérez-Gutiérrez L and Ferrara N: Biology and therapeutic targeting of vascular endothelial growth factor A. Nat Rev Mol Cell Biol 24: 816-834, 2023.
42. Vornic I, Buciu V, Furau CG, Gaje PN, Ceausu RA, Dumitru CS, Barb AC, Novacescu D, Cumpanas AA, Latcu SC, *et al*: Oxidative stress and placental pathogenesis: A contemporary overview of potential biomarkers and emerging therapeutics. Int J Mol Sci 25: 12195, 2024.
43. Knöfler M, Haider S, Saleh L, Pollheimer J, Gamage TKJB and James J: Human placenta and trophoblast development: Key molecular mechanisms and model systems. Cell Mol Life Sci 76: 3479-3496, 2019.
44. Murray AJ: Oxygen delivery and fetal-placental growth: Beyond a question of supply and demand? Placenta 33 (Suppl 2): e16-e22, 2012.
45. Ducsay CA, Goyal R, Pearce WJ, Wilson S, Hu XQ and Zhang L: Gestational hypoxia and developmental plasticity. Physiol Rev 98: 1241-1334, 2018.
46. Su EJ, Xin H, Yin P, Dyson M, Coon J, Farrow KN, Mestan KK and Ernst LM: Impaired fetoplacental angiogenesis in growth-restricted fetuses with abnormal umbilical artery doppler velocimetry is mediated by aryl hydrocarbon receptor nuclear translocator (ARNT). J Clin Endocrinol Metab 100: E30-E40, 2015.
47. Carr DJ, David AL, Aitken RP, Milne JS, Borowicz PP, Wallace JM and Redmer DA: Placental vascularity and markers of angiogenesis in relation to prenatal growth status in overnourished adolescent ewes. Placenta 46: 79-86, 2016.
48. Hu C, Yang Y, Deng M, Yang L, Shu G, Jiang Q, Zhang S, Li X, Yin Y, Tan C and Wu G: Placentae for low birth weight piglets are vulnerable to oxidative stress, mitochondrial dysfunction, and impaired angiogenesis. Oxid Med Cell Longev 2020: 8715412, 2020.
49. Hu C, Wu Z, Huang Z, Hao X, Wang S, Deng J, Yin Y and Tan C: Nox2 impairs VEGF-A-induced angiogenesis in placenta via mitochondrial ROS-STAT3 pathway. Redox Biol 45: 102051, 2021.
50. Wu Z, Nie J, Wu D, Huang S, Chen J, Liang H, Hao X, Feng L, Luo H and Tan C: Dietary adenosine supplementation improves placental angiogenesis in IUGR piglets by up-regulating adenosine A2a receptor. Anim Nutr 13: 282-288, 2023.
51. Lanng MB, Møller CB, Andersen ASH, Pálsdóttir AA, Røge R, Østergaard LR and Jørgensen AS: Quality assessment of Ki67 staining using cell line proliferation index and stain intensity features. Cytometry A 95: 381-388, 2019.
52. Bullwinkel J, Baron-Lühr B, Lüdemann A, Wohlenberg C, Gerdes J and Scholzen T: Ki-67 protein is associated with ribosomal RNA transcription in quiescent and proliferating cells. J Cell Physiol 206: 624-635, 2006.
53. Li C, Xiao N, Song W, Lam AHC, Liu F, Cui X, Ye Z, Chen Y, Ren P, Cai J, *et al*: Chronic lung inflammation and CK14+ basal cell proliferation induce persistent alveolar-bronchiolization in SARS-CoV-2-infected hamsters. EBioMedicine 108: 105363, 2024.
54. Devi K, Tomar MS, Barsain M, Shrivastava A and Moharana B: Regeneration capability of neonatal lung-derived decellularized extracellular matrix in an emphysema model. J Control Release 372: 234-250, 2024.
55. Xinqiang Y, Quan C, Yuanyuan J and Hanmei X: Protective effect of MOTS-c on acute lung injury induced by lipopolysaccharide in mice. Int Immunopharmacol 80: 106174, 2020.
56. Wu F, Tian FJ and Lin Y: Oxidative stress in placenta: Health and diseases. Biomed Res Int 2015: 293271, 2015.
57. Biri A, Bozkurt N, Turp A, Kavutcu M, Himmetoglu O and Durak I: Role of oxidative stress in intrauterine growth restriction. Gynecol Obstet Invest 64: 187-192, 2007.
58. Hu XQ and Zhang L: Hypoxia and Mitochondrial dysfunction in pregnancy complications. Antioxidants (Basel) 10: 405, 2021.
59. Kaandorp JJ, Benders MJNL, Schuit E, Rademaker CM, Oudijk MA, Porath MM, Oetomo SB, Wouters MG, van Elburg RM, Franssen MT, *et al*: Maternal allopurinol administration during suspected fetal hypoxia: A novel neuroprotective intervention? A multicentre randomised placebo controlled trial. Arch Dis Child Fetal Neonatal Ed 100: F216-F223, 2015.

60. Klumper J, Kaandorp JJ, Schuit E, Groenendaal F, Koopman-Esseboom C, Mulder EJH, Van Bel F, Benders MJNL, Mol BWJ, van Elburg RM, *et al*: Behavioral and neurodevelopmental outcome of children after maternal allopurinol administration during suspected fetal hypoxia: 5-year follow up of the ALLO-trial. PLoS One 13: e0201063, 2018.
61. Rashid CS, Bansal A and Simmons RA: Oxidative stress, intrauterine growth restriction, and developmental programming of type 2 diabetes. Physiology (Bethesda) 33: 348-359, 2018.
62. Shaw P and Chattopadhyay A: Nrf2-ARE signaling in cellular protection: Mechanism of action and the regulatory mechanisms. J Cell Physiol 235: 3119-3130, 2020.
63. Zhou H, Wang Y, You Q and Jiang Z: Recent progress in the development of small molecule Nrf2 activators: A patent review (2017-present). Expert Opin Ther Pat 30: 209-225, 2020.
64. Acar N, Soylu H, Edizer I, Ozbey O, Er H, Akkoyunlu G, Gemici B and Ustunel I: Expression of nuclear factor erythroid 2-related factor 2 (Nrf2) and peroxiredoxin 6 (Prdx6) proteins in healthy and pathologic placentas of human and rat. Acta Histochem 116: 1289-1300, 2014.
65. Chen S, Yin Q, Hu H, Chen Q, Huang Q and Zhong M: AOPPs induce HTR-8/SVneo cell apoptosis by downregulating the Nrf-2/ARE/HO-1 anti-oxidative pathway: Potential implications for preeclampsia. Placenta 112: 1-8, 2021.
66. Gao Y, Wei X, Wei P, Lu H, Zhong L, Tan J, Liu H and Liu Z: MOTS-c functionally prevents metabolic disorders. Metabolites 13: 125, 2023.
67. Knoop A, Thomas A and Thevis M: Development of a mass spectrometry based detection method for the mitochondrion-derived peptide MOTS-c in plasma samples for doping control purposes. Rapid Commun Mass Spectrom 33: 371-380, 2019.